

# Tau Air Showers from Earth

D. Fargion<sup>1,2</sup>, P.G. De Sanctis Lucentini<sup>1</sup>, M. De Santis<sup>1</sup>, M.Grossi<sup>1</sup>

<sup>1</sup> Physics Department, Università "La Sapienza", Pl.A.Moro, <sup>2</sup> INFN, Rome, Italy

Received \_\_\_\_\_; accepted \_\_\_\_\_

arXiv:hep-ph/0305128v4 16 Apr 2004

---

<sup>1</sup>Physics Department, Università "La Sapienza", P.le A.Moro 5, 00185 Roma, Italy

<sup>2</sup>INFN Roma1, Italy

## ABSTRACT

We estimate the rate of observable Horizontal and Upward Tau Air-Showers (HORTAUs, UPTAUS) considering both the Earth opacity and the contribution of the terrestrial atmosphere. Our result applies to most neutrino telescope projects especially to the EUSO space observatory. Using a compact analytical formula we calculate the effective target volumes and masses for Tau air-showers emerging from the Earth. The resulting model-independent effective masses for EUSO may encompass - at  $E_{\nu_\tau} \simeq 10^{19}$  eV - an average huge volume ( $\simeq 1020$   $km^3$ ) compared to current neutrino experiments. Adopting simple power law neutrino fluxes,  $\frac{dN_\nu}{dE_\nu} \propto E^{-2}$  and  $E^{-1}$ , calibrated to GZK-like and Z-Burst-like models, we estimate that at  $E \simeq 10^{19}$  eV nearly half a dozen horizontal shower events should be detected by EUSO in three years of data collection considering the 10% duty cycle efficiency and a minimal  $\nu_\tau$  flux  $\phi_\nu E_\nu \simeq 50 \text{eV cm}^{-2} \text{ s}^{-1} \text{ sr}^{-1}$ . The HORTAUS detection may test the "guaranteed" GZK neutrino flux (secondaries of photopion production due to UHECR scattering onto 2.75 K cosmic background radiation). We also find that the equivalent mass for an outer layer made of rock is dominant compared to the water, contrary to simplified all-rock/all-water Earth models and previous studies. Therefore we expect an enhancement of neutrino detection along continental shelves nearby the highest mountain chains, also because of the better geometrical acceptance for Earth skimming neutrinos. In this picture, the Auger experiment might reveal such an increase at  $E_\nu \simeq 10^{18}$  eV (with 26 events in 3 yr) if the angular resolution (both in azimuth and zenith) would reach an accuracy of nearly one degree necessary to disentangle tau air showers from common horizontal UHECR. Finally, we show that the number of events increases at lower energies, therefore we suggest an extension of the EUSO sensitivity down to  $E_\nu \sim 10^{19}$  eV or even below.

## 1. Introduction: $\tau$ air-showering from the Earth

The study of ultrahigh energy upward and horizontal  $\tau$  air showers produced by  $\tau$  neutrino interactions within the Earth crust has been considered in recent years as an alternative way to detect high energy neutrinos. The problem of  $\tau$  neutrinos crossing the Earth is indeed quite complicated because of the complex terrestrial neutrino opacity at different energies and angles of arrival. In addition, several factors have to be taken into account, such as the amount of energy transferred in the  $\nu_\tau$  -  $\tau$  lepton conversion, as well as the  $\tau$  energy losses and interaction lengths at different energies and materials. This makes the estimate of the links between the input neutrino - output  $\tau$  air shower very difficult. Such a prediction is further complicated by the existence of a long list of theoretical models for the incoming neutrino fluxes (GZK neutrinos, Z-burst model flux,  $E^{-2}$  flat spectra, AGN neutrinos, topological defects). Many authors have investigated this mechanism, however the results are varied, often in contradiction among themselves, and the expected rates range over a few order of magnitude (Fargion, Aiello, & Conversano 1999; Fargion 2002a; Feng et al. 2002; Bottai & Giurgola, hereafter BG03; Bugaev, Montaruli, & Sokalski 2003; Fargion 2003; Tseng et al. 2003; Jones et al. 2004; Yoshida et al. 2004). So far, the majority of the current studies on this topic is based on Monte-Carlo simulations assuming a particular model of the incoming neutrino flux.

To face such a complex problem, we think that the simplest approach is the best. First one has to disentangle the incoming neutrino flux from the consequent  $\tau$  air-shower physics. Therefore, to establish the  $\tau$  production rate we introduce an effective volume and mass for Earth-skimming  $\tau$ 's, which is independent on any incoming neutrino flux model. This volume describes a strip within the Earth where neutrino/antineutrino-nucleon,  $\nu_\tau(\bar{\nu}_\tau) - N$ ,

interactions may produce emerging  $\tau^-$ ,  $\tau^+$  leptons which then shower in air.

We present a very simple analytical and numerical derivation (as well as its more sophisticated extensions) which takes into account, for any incoming angle, the main processes related to the neutrinos and  $\tau$  leptons propagation and the  $\tau$  energy losses within the Earth crust. Our numerical results are constrained by upper and lower bounds derived in simple approximations (enlisted in a final appendix). The effective volumes and masses will be more severely reduced at high energy because we are interested in the successful development of the  $\tau$  air-shower. Therefore we included as a further constraint the role of the air dilution at high altitude, where  $\tau$  decay and the consequent air-shower may (or may not) take place.

We show that our results give an estimate of the  $\tau$  air-shower event rates that greatly exceeds earliest studies but they are comparable or even below more recent predictions. To make our derivation as simple as possible we present only the main formula and plots, while full details of the calculations and of the approximation limits will be discussed in the appendix.

We compare our general  $\tau$  upward-going showers to detectors such as the ongoing photo-fluorescence ground-based observatory Auger, we present some definitive predictions for future projects like the EUSO space observatory and we suggest how to enhance the neutrino tau emergence especially at energies lower than  $10^{19}$  eV.

The paper is divided in the following way: section §2 gives a brief review of the expected Ultra High Energy Neutrino Sources. Section §3 discusses the general air-shower neutrino telescope scenario focusing on  $\tau$  Neutrino Astronomy, with a minor hint to the present and future underground  $km^3$  neutrino detectors; in section §4 we introduce the comparable horizontal Ultra High Energy Cosmic Rays Air-Skimming events at high altitude (HIAS) and the lower air-skimming neutrino induced air-shower; we calculate the Earth opacity

for neutrinos and leptons; we briefly remind the lepton energy losses in different materials (water and rock), and we present the effective Earth skin Volumes and Masses leading to UPTAUs and HORTAUs. Such volumes and masses will be derived under different approximations and experimental framework. In section §5 we present the event rate per  $\text{km}^2$  assuming that the outer layer of the Earth’s crust is made either of rock or of water and we compare it with large area projects such as Auger and EUSO. Section §6 will show our conclusions and suggestions for  $\tau$  air-shower Neutrino Astronomy, mainly concentrating on the EUSO experiment.

## 2. Sources of High Energy Neutrinos

### 2.1. The atmospheric neutrinos background

Cosmic Rays (CR) reach the Earth’s atmosphere with a nearly homogeneous and isotropic distribution with no astronomical memory of their original place of birth. Parasite secondary neutrinos originated by such blurred CR are abundantly hitting the atmosphere, leading to an atmospheric neutrino background, with the same nearly isotropic distribution as the parental CR flux in celestial coordinates (with a power law spectrum  $\propto E^{-2.2}$ ). Their presence is a polluting signal for any future Neutrino Astronomy. Nevertheless the atmospheric neutrino background is suppressed at high energy ( $E_{\nu_{Atm}} > TeV$ ) and shows a spectrum ( $\propto E^{-3.2}$ ) softer than that of the parental CR, because the relativistic charged pion lifetime is larger than the time needed to propagate through the atmosphere, and they do not easily decay neither into muons nor into atmospheric neutrinos. Therefore the detection of High Energy Neutrinos from galactic or extragalactic objects is expected above  $\sim 10$  TeVs (i.e. PeV - EeV - ZeV) assuming a harder spectrum for neutrinos from astronomical sources. It is worth noticing that the TeV-PeV charged cosmic rays are confined within the Galaxy by the magnetic field, thus they are more long-lived and tangled

than direct galactic neutrinos; this makes more likely (by at least two-three orders of magnitude) the detection of atmospheric  $\nu$ 's (produced by galactic CR) compared to those neutrinos from astrophysical sources, whose harder spectrum may compensate this large difference.

At high energy ( $> 10^{19}$  eV) CR losses are also of nuclear nature (photo-pion and multi-pion productions) and Ultra High Energy Cosmic Rays, UHECR, mainly nuclei and nucleons, often produce charged pions leading to neutrino and gamma secondaries nearby the original source, such as an Active Galactic Nucleus (AGN). In this case we may expect an UHE neutrino astronomy (at EeV-PeV) associated with such UHECR and with hard gamma photons, secondaries of neutral pions (Semikoz & Sigl 2003). Such UHE neutrinos are often labeled as AGN secondary neutrinos. While they travel undeflected and unperturbed, the corresponding gamma are often absorbed and degraded to GeV - MeV energies by intergalactic backgrounds.

In the following sections we summarize the main sources of primary UHE neutrinos such as the AGN, Gamma Ray Bursts (GRB) or more exotic topological defects (TD), as well as the production of secondary  $\nu$ 's by UHECR at GZK energies (GZK or cosmogenic neutrino) and UHE neutrons. We also discuss the role of UHE neutrinos as sources of UHECRs via  $\nu - \nu_{relic}$  scattering, as predicted by the Z-burst scenario.

## 2.2. UHE $\nu$ correlated to UHE neutrons

Neutral EeV neutrons may trace a corresponding neutrino imprint through their beta decay in flight. Recently, a mild correlation has been found between the Cosmic Ray excess in the AGASA data at EeV energies with the EGRET gamma map towards Cygnus and the Galactic Omega 17 region (Hayashida et al. 1999; Fargion 2002a; Fargion, Khlopov et

al. 2003). The nature of such EeV galactic anisotropy cannot be related to charged cosmic rays at high EeV rigidity but it may be due to EeV neutrons - able to avoid the galactic magnetic field bending and to survive up to galactic distances  $D_n = 9.168 \cdot \left(\frac{E_n}{10^{18} \text{eV}}\right) \cdot \text{kpc}$ . These UHECR neutrons anisotropy at 4% level would imply an associated UHE neutrino flux. Indeed neutrinos might be either the inescapable low tail of neutron decay in flight, or the signature of UHE pions generated in the same source with the UHE neutrons. In the first case (relic of neutron's beta decay in flight) the expected secondary neutrino energy flux is a negligible ( $\leq 1\%$ ) fraction of UHE neutron:  $\phi_\nu \ll 12 \text{ eV cm}^{-2} \text{ s}^{-2} \text{ sr}^{-2}$ ; while in the latter case (assuming the equipartition of the energy into pion-neutron "in situ" production) the expected neutrino flux near EeV might exceed (up to a factor ten) the UHE neutron flux  $\phi_\nu \simeq 100 \text{ eV cm}^{-2} \text{ s}^{-2} \text{ sr}^{-2}$ .

### 2.3. UHE neutrinos from AGN and GRB

UHECR escaping from a Jet of a Quasar (QSO) or an AGN, or a beamed GRB - Supernova (SN) Jet may interact with the intense photon fields generated by the source itself. These interactions lead to the production of charged and neutral mesons fuelling a collinear gamma and neutrino flux (Kalashev et al. 2002). The gamma rays and the high energy cosmic rays may interact inside the much denser environment of the source (AGN,GRB Jets) where the gamma opacity suppresses most of the electromagnetic escaping signal. In this scenario the main signal coming from the core of AGN might be dominated by 'transparent' Ultra High Energy Neutrinos whose fluxes may be even greater than the gammas. These AGN or GRB-SN Jet neutrinos have been often modeled and predicted in the PeV-EeV energy range, and they may be well correlated with gamma photons produced by blazars, if they are originated by the interactions of relativistic nuclei. EeV photons by neutral pion decay are suppressed by photon-photon interactions and their energy may be

degraded to MeV-GeV energies. The neutrino energy fluence may reach a value comparable or just below the one of the diffuse gammas observed by EGRET:  $\phi_\nu \simeq 10^3 \text{ eV cm}^{-2}\text{s}^{-2}\text{sr}^{-2}$ . The slope of the spectrum near the maximum at PeV energy might be flat:  $\phi_\nu \propto E^{-2}$ .

#### 2.4. UHE GZK neutrinos and the Z burst: neutrino masses imprint

The origin of UHECRs with energies above a few times  $10^{19}$  eV is a phenomenon that has not yet been clearly understood. There are nearly a hundred of such UHECR events, which surprisingly are not clustered to any nearby AGN, QSRs or known GRBs within the narrow volume (10-30 Mpc radius) defined by the cosmic  $2.75 K^o$  proton drag viscosity, the so-called GZK cut-off (Greisen 1966; Zatsepin & Kuzmin 1966). Indeed the GZK cut-off implies the shrinking of the UHECR propagation length to a few tens of Mpc, making the expected UHECR astronomy a very local one. However these events are neither correlated with any galactic or nearby Local Group sources, nor with the Super-Galactic plane, nor with nearby clusters. Following the Gamma Ray Burst lesson, the observed UHECR overall isotropy is suggesting a very far away cosmological origin. Such cosmic distances are not consistent with the  $< 10$  Mpc cut-off prescribed by the GZK effect. Moreover, the presence of a few UHECR clustered events, apparently correlated with a more distant, bright BL Lac population makes this puzzle even more complicated. Such BL Lac objects are in fact at far redshifts ( $z > 0.1 - 0.3$ ) (Gorbunov, Tinyakov, Tkachev, Troitsky 2002). This correlation and the overall isotropy favor a cosmic origination for UHECRs, well above the near GZK volume.

A light ( $0.05 \text{ eV} < m_\nu < 2 \text{ eV}$ ) relic neutrino may play a role in solving the puzzle. Assuming a neutrino flux at corresponding energies ( $2 \cdot 10^{21} \text{ eV} < E_\nu < 8 \cdot 10^{22} \text{ eV}$ ) ejected by distant BL Lacs, such UHE  $\nu$ 's may be hitting relic light neutrinos clustered in Hot Dark Halos with a characteristic size of a few Mpc (for instance as extended as the Local



Group) or of tens of Mpc (the supergalactic cluster volume). This interaction produces an UHE Z boson (Z-Shower or Z Burst model) whose secondary nucleons are the final observed UHECRs on Earth. In synthesis, the UHE neutrino is the neutral flying link (transparent to BBR photons) from BL Lac sources at cosmic edges to our local universe, while the relic neutrinos, possibly clustered in Mpc or ten Mpc volumes around the Local Group, represent the target calorimeter. In this scenario, a neutrino mass (Dolgov 2002; Raffelt 2002) fine-tuned at  $m_\nu \simeq 0.4$  eV (Fargion, Grossi et al. 2000, 2001; Fodor, Katz, Ringwald 2002; Klapdor-Kleingrothaus et al. 2001) or  $m_\nu \simeq 0.1 \div 5$  eV, may solve the GZK paradox overcoming the proton opacity. (Fargion, Salis, 1997; Fargion, Mele, & Salis 1999; Yoshida et al 1998; Weiler 1999). In order to fit the UHECR observed data a UHECR Z-burst neutrino flux at  $E \simeq 10^{19} eV$  should grow as  $\phi_\nu \simeq 50 \cdot E^{-1} eV cm^{-2} s^{-1} sr^{-1}$ .

Therefore, UHE neutrinos may induce, as primary particles, the astronomy of the UHECRs and their detection may allow to identify the sources where such UHE particles are produced. Yet, independently on the exact GZK puzzle solution, the extragalactic UHE nucleons produced in our GZK surrounding are themselves source of UHE neutrinos  $\nu_\mu, \bar{\nu}_\mu, \nu_e, \bar{\nu}_e$ , with energies  $E \simeq 4 \cdot 10^{19} eV$ , and UHE gammas by photopion production.

However, the light neutrino mass required to avoid the GZK paradox does not solve the dark matter problem, although it is well consistent with the solar neutrino oscillation mass limits (Anselmann et al. 1992; Fukuda 1998), with the most recent claims of anti-neutrino disappearance by KamLAND (Eguchi et al. 2003) (in agreement with a Large Mixing Angle neutrino model and  $\Delta m_\nu^2 \sim 7 \cdot 10^{-5} eV^2$ ), and with the atmospheric neutrino mass splitting ( $\Delta m_\nu \simeq 0.07$  eV). Finally, a light neutrino mass in agreement with the Z-burst model (Fargion, Grossi et al. 2000, 2001) may be compatible with the more recent (but controversial) results from the neutrino double beta decay, which sets the mass at  $m_\nu \simeq 0.4$  eV (Klapdor-Kleingrothaus 2002).

## 2.5. Topological defects

Current theories of particle physics predict that a variety of topological defects have formed during the early stages of the evolution of the universe. Such extremely heavy relic particles, indicated as monopoles, strings, walls or necklaces, might be originated as fossil remnants of phase transitions occurring at the Grand Unified Theories energy scale of  $10^{15}$  GeV. The potential role of topological defects as an alternative explanation to the origin of UHECRs above  $10^{20}$  eV has been proposed and investigated in the recent years (Bhattacharjee, Hill, & Schramm 1992; Sigl, Schramm, & Bhattacharjee 1994). Their decay lifetime is somehow fine-tuned with the Universe age. In addition, pair annihilations of heavy particles (TD-like), born in bounded binary system, might also be a viable processes in a narrow parameter range (Dubrovich, Fargion & Khlopov 2004). It is not clear if there are any sites in the universe capable to accelerate the observed particles at such high energies, while the annihilation and decay of topological defects may produce prompt extremely high energy cosmic rays and neutrinos. The search for such neutrinos reaching the energy of GUT scale may shed light on these models and theories. However, even if the TD scenario may solve the puzzle of the particles' acceleration, the clustering of some UHECR events (doublets or triplets) is hardly explicable by the decay of a diffuse halo distribution of superheavy particles (Uchihori et al. 2000, Tinyakov, & Tkachev 2001). Such UHE neutrino spectra from TD might follow a power law  $\propto E^{-3/2}$  in between the Z-burst  $\propto E^{-1}$  and GZK  $\propto E^{-2}$  power laws.

## 3. UHE Neutrino Telescopes: Electron, Muon and Tau traces in underground ice-water and air detectors

The very possible discover of an UHECR astronomy, the solution of the GZK paradox, the very urgent rise of an UHE neutrino astronomy are among the main goals of many new

neutrino telescope projects. Most detectors are related to the muon track in underground  $Km^3$  volumes, either in water or ice (Halzen, & Hooper 2002). Such detectors consist of a lattice of photo-multipliers spread over large volumes and look for high energy neutrinos from the Cherenkov emission of muons produced in  $\nu - N$  interactions. The detectors select preferentially upward-going muons entering from below, originated by neutrinos propagating through the Earth, while the vertical downward-going signals are polluted by atmospheric muons. DUMAND and later BAIKAL detectors have been the pioneer projects of under-ice detectors, more recently implemented by AMANDA (Andres et al. 1997) and its extensions AMANDA II at the South Pole, with 677 photo-multipliers placed in the ice at depths between 1500 and 2000 meters.

ANTARES (Montaruli et al. 2002) and NESTOR (Grieder et al. 2001) in the Mediterranean sea, are the two ongoing projects for under-water telescopes planned to be finished by 2006. Other detectors are related to the UHE neutrino showering in air. The UHE neutrino interactions lead to nuclear or electromagnetic showers. The UHE neutrino-nuclei charged current interactions may produce electrons, muons or taus in air and/or water. In underground detectors the electron-muon-tau interactions are leading to a Cherenkov flash with or without a lepton track. Muon tracks are the most penetrating at energies  $\leq 10^{18}$  eV, while taus are more penetrating, as we shall see, at higher energies. The underground detectors are not aimed at disentangling the lepton nature of the tracks.

Among the experiments on the ground, Auger is designed to detect air-showers both by muons bundles and their fluorescence lights for downward UHECR. Auger will investigate the region of the CR spectrum around the GZK cut-off; however the characteristics of the observatory are such that it may be able to detect also HORTAUs events. The well amplified horizontal air-shower at a slant depth larger than  $2000g\text{ cm}^{-2}$ , (but not exceeding  $\gg 10^4 - 3 \cdot 10^4\text{ g cm}^{-2}$ ), may trace an induced neutrino air-shower event originated in air

or, at higher rate, an air-shower due to Tau decay in flight (HORTAUs) triggered by an interaction within the nearby Andes mountain chain (Fargion, Aiello, & Conversano 1999; Fargion 2002a; Bertou et al. 2002) or emerging directly from the Earth crust. We will discuss this possibility in the following sections.

Auger is under construction in Argentina, it is planned to be completed by 2005/2006 and it will be operative for about a decade. It is the first prototype of a hybrid observatory for the highest energy cosmic rays consisting of both a surface array of particle detectors and fluorescence telescopes looking at the Cherenkov emission from high energy charged particles propagating through the atmosphere. It will have an aperture of  $7 \times 10^3 \text{ km}^2 \text{ sr}$ , which is roughly a factor 10 larger than HiRes. The observatory includes also an analogue counterpart in the northern hemisphere which will allow full sky coverage in order to study in detail the spatial distribution of such events.

Another competitive experiment is EUSO due to be launched in a very near future. The EUSO detector is a wide angle UV telescope that will be placed on the International Space Station (ISS). It will look, in dark time, downward towards the Earth atmosphere, and its aperture is such to cover a surface as large as  $\sim 1.6 \times 10^5 \text{ Km}$ . Therefore it will encompass AGASA-HIRES and Auger areas as well as their rate of UHECR events (Cronin 2004). EUSO is designed to detect and measure fluorescence and Cherenkov photons produced by the interactions of UHECR in the atmosphere. As cosmic rays penetrate the atmosphere they may originate both a photo-fluorescence signal (due to the excitation of  $N_2$  molecules) and a secondary (albedo) reflection by Cherenkov photons. Given the large amount of UV radiation emitted by the  $N_2$  molecules, a substantial fraction of UV photons is expected to reach the detector outside the Earth's atmosphere at a height of  $\sim 400 \text{ km}$ . For instance, for a  $10^{20} \text{ eV}$  extended air shower (EAS), a few thousand of photons are expected to reach EUSO . A much larger number (at least two order of magnitude)

of Cherenkov diffused photons are expected for High Altitude Air-Showers (HIAS) and HORTAUs. We will discuss in detail in the following sections the possibility for EUSO to detect Horizontal Tau Air-Showers originated within a very wide terrestrial skin volume around its field of view (FOV)

As mentioned in section §2, the scattering of UHE neutrino onto light relic neutrinos may solve the GZK paradox as predicted by the Z-burst model. EUSO will play an important role to discriminate between different scenarios proposed for the origin of UHECR and it may discover UHE neutrino signals due to the Z burst or due to the "guaranteed" GZK ones.

#### 4. UHE $\nu$ Astronomy by the Upward $\tau$ Air-Showering

While longest  $\mu$  tracks in  $km^3$  underground detector have been, in last three decades, the main searched UHE neutrino signal, tau air-showers by UHE neutrinos generated in mountain chains or within the Earth skin crust at PeV up to GZK energies ( $> 10^{19}$  eV) have been recently proved to be a powerful amplifier in Neutrino Astronomy (Fargion, Aiello, & Conversano 1999; Fargion 2002a; Bertou et al. 2002; Hou Huang 2002; Feng et al 2002). Indeed up-going UHE muons  $E_\mu \geq 10^{14}$  eV, born from upward or Earth skimming muon neutrinos, will propagate and escape from the Earth atmosphere without any significant air-shower trace,  $L_\mu = 6.6 \cdot 10^{10} \text{ cm} \left( \frac{E_\mu}{10^{14} \text{ eV}} \right) \gg$  atmosphere height. The UHE electron produced by UHE  $\nu_e$  will shower mainly within a very thin terrestrial crust and its event will remain generally hidden and "buried" inside the Earth. On the contrary UHE  $\tau$  by UHE  $\nu_\tau - N$  interactions are able to cross thick earth crust layers and they might emerge freely from the Earth. The short  $\tau$  lifetime will lead to a decay in flight and to an amplified air-showering at tuned  $10^{14} - 10^{19}$  eV energy band, within the main interesting astrophysical range.

Neutrino  $\tau$  detectors searching for UPTAUs and HORTAUs will be (at least) complementary to present and future, lower energy underground  $km^3$  telescope projects (such as AMANDA, Baikal, ANTARES, NESTOR, NEMO, IceCube). In particular Horizontal Tau Air shower may be naturally originated by UHE  $\nu_\tau$  at GZK energies crossing the Earth Crust just below the horizon and/or nearby high mountain chains as the Andes. UHE  $\nu_\tau$  are abundantly produced by flavour oscillation and mixing from muonic (or electronic) neutrinos, since galactic and cosmic distances are larger than the neutrino oscillation lengths  $L_{\nu_\mu-\nu_\tau} = 2.48 \cdot 10^{19} \text{ cm} \left( \frac{E_\nu}{10^{19} \text{ eV}} \right) \left( \frac{\Delta m_{ij}^2}{(10^{-2} \text{ eV})^2} \right)^{-1} \simeq 8.3pc$ . Therefore EUSO may observe HORTAUs events and it may set constraint on models and fluxes, possibly answering some open questions. Let us first describe the background UHECR events able to mimic the HORTAUs signal that we are considering here.

Figure 1 displays a characteristic scenario where a common UHECR hits horizontally the Earth atmosphere leading to a high altitude Air-Shower (HIAS, or Albedo Shower). This event takes place at an altitude of  $\sim 40$  km. A more interesting but similar air-shower might originate at higher atmospheric density, i.e. at altitudes lower than 10 km, by weak interacting neutrinos hitting the air nuclei. These events might be better detected by most present arrays or satellites at high energies  $\sim 10^{19}$ eV. Figure 2 describes the Horizontal Tau Air-Shower, HORTAUs event at  $\sim 10^{18} - 10^{19}$  eV energy range below the horizon, whose detection efficiency is not contaminated by any downward cosmic ray background. Finally on the right-hand side of Figure 2 we describe a much lower energy  $\sim 10^{14} - 10^{17}$  eV Upward Tau Air-Shower UPTAUs induced as for HORTAUs by incoming tau neutrino able to cross the Earth inclined or almost vertical. At energies  $leq 2 \cdot 10^{14}$  eV and below the UPTAUs more often take place inside the terrestrial atmospheric layer.

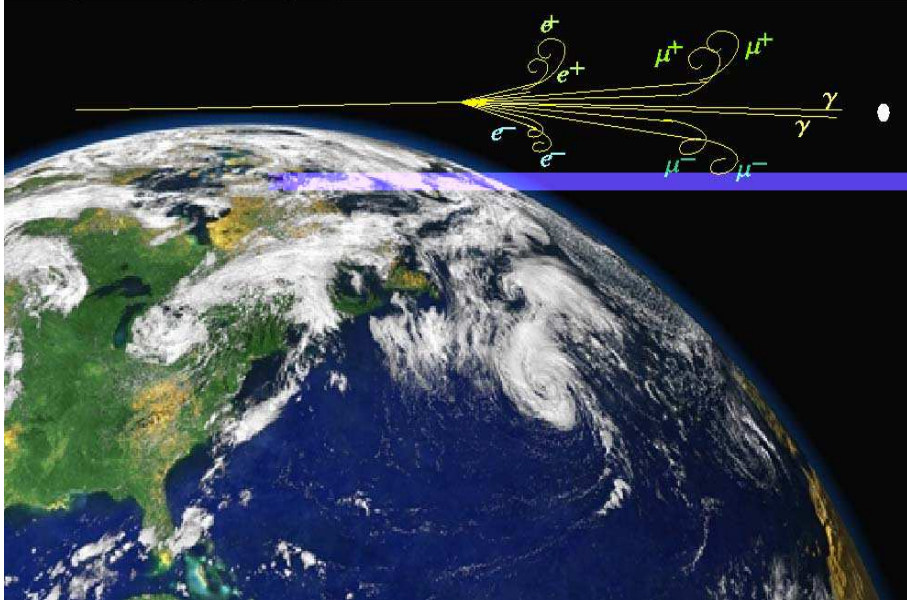


Fig. 1.— A very schematic Horizontal High Altitude Shower (HIAS); UHECRs (nucleon or nuclei or gamma) interact with the atoms of the atmosphere at high altitude, producing a fan-shaped air-shower due to the geo-magnetic bending of charged particles (mainly lepton pairs) at high quota ( $\sim 44km$ ). The Shower may point to a satellite as the old gamma GRO-BATSE detectors or to the more recent Beppo-Sax, Integral, HETE, Chandra or the future ones as Agile, Swift and GLAST (Fargion 2001b, 2001c, 2002a). These HIAS Showers are extremely long (hundred km size) and they are often split in five (or three) main components:  $e^+ e^-, \mu^+ \mu^-, \gamma$ . Such multiple tails may be detected in long horizontal air-showers by EUSO, and they may be distinguished by their orthogonality to the local magnetic fields. At much lower altitude, below 10 km height, there are very similar UHE horizontal showers due to neutrino-air interactions leading to Neutrino Induced Air-Showers at slant depth  $X_{max} \gg 10^3 gcm^{-2}$

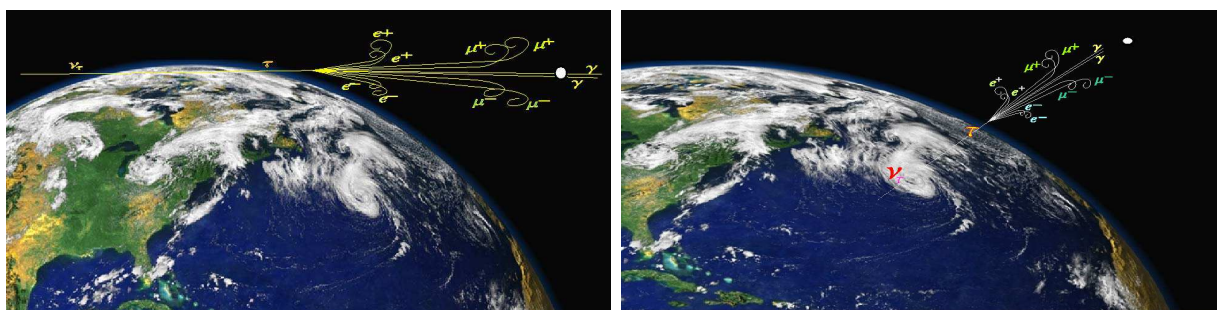


Fig. 2.— **left**) Horizontal Upward Tau Air-Shower (HORTAUS) originated by UHE neutrino skimming the Earth: fan-shaped jets arise because of the geo-magnetic bending of charged particles at high quota ( $\sim 23 - 40$  km). The shower signature may be observable by EUSO just above the horizon. Because of the Earth opacity most of the UPTAU events at angles  $\theta > 45 - 50^\circ$  will not be observable, since they will not be contained within its current field of view (FOV). **right**) A very schematic UPTAU air-shower at high altitude ( $\sim 20-30$  km). The vertical tail may be spread by geo-magnetic field into a thin eight-shaped beam, observable by EUSO as a small blazing oval (few dot-pixels) orthogonal to the local magnetic field.



#### 4.1. Effective Volume

Let us define two main effective volumes below the Earth surface where UPTAUs and HORTAUs might originate:

1. A deeper skin volume which is defined by all possible  $\nu_\tau$ 's whose secondary  $\tau$ 's tracks escape from the Earth. This volume is obtained by considering the Earth opacity to the incoming neutrinos and the inelasticity factor in the conversion  $\nu_\tau \rightarrow \tau$ , disregarding the exact outgoing  $\tau$  final energy. In this case the  $\tau$  propagation (or interaction) length, to be estimated in the following section,  $l_\tau$  is defined uniquely by the incoming neutrino energy  $E_{\nu_\tau}$  and by the energy losses in matter (see Fig. 3).
2. A thinner skin volume whose size may be defined by the outgoing  $\tau$  energy ( which is related to the primary  $\nu_\tau$  energy). In this calculation we take into account the earth's opacity, and the average energy losses of  $\tau$  leptons traveling through the earth's crust and escaping into the atmosphere. The  $\tau$  air-shower generation depends on the presence of the atmosphere, whose thickness defines an additional suppression at highest energies. In this case the  $\tau$  propagation (or interaction) length  $L_{\tau(\beta)}$  (see next section) is much shorter than the  $l_\tau$  length (see Fig. 3).

Between these two scenarios, different effective volumes may be obtained as a function of the primary neutrino energy  $E_{\nu_{\tau_i}}$  or the newly born  $\tau$  ( $E_{\tau_i}$ ) or the final  $\tau$  energy ( $E_{\tau_f}$ ) related to the observed air-shower; such different possibilities may lead to ambiguities in the meaning and in the prediction of the UPTAUs and HORTAUs rates. Many authors calculate the UPTAUs rates as a function of the incoming neutrino energy  $E_{\nu_{\tau_i}}$ . In the present article we calculate the Volumes, Masses and Rates as a function of both the primary neutrino energy and the final tau energy. This procedure avoids ambiguities and allows an easier comparison with other studies.

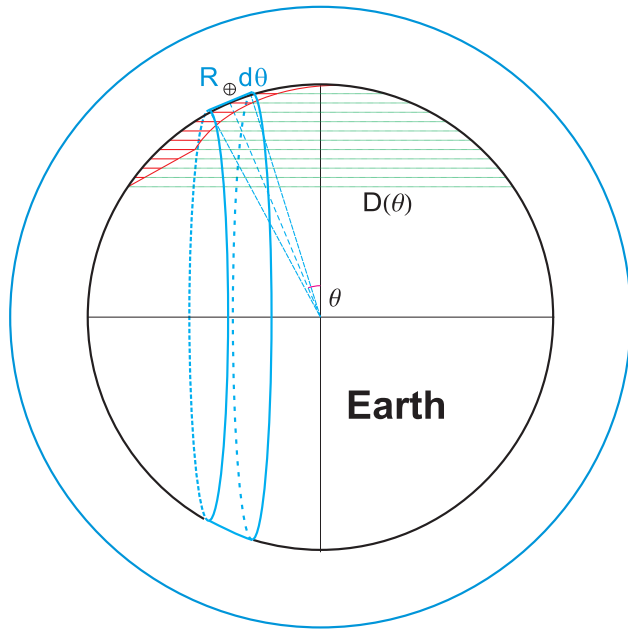


Fig. 3.— A schematic representation of the possible incoming neutrino trajectory through the Earth with the consequent production of a tau lepton track. The thin shaded area on the left (just below the Earth) defines the volume where the interaction occurs. This area might be thinner for  $L_{\tau(\beta)}$  than for  $l_{\tau}$  interaction length. These emerging  $\tau$ 's may decay in flight, producing the HORTAUs within the terrestrial atmosphere.

As we previously mentioned, our final effective volume should be suppressed by a factor that includes the finite extension of the earth's atmosphere (both for vertical and inclined air-showers) which has never been considered before. This suppression guarantees that one deals with only a fully developed air-shower and that  $\tau$  decays outside the terrestrial atmosphere are discarded.

When one calculates the neutrino propagation through the Earth one should take into account the complex internal structure of our planet. Generally this may be approximated as a sphere consisting of a number of layers with different densities, as represented in the Preliminary Earth Model (Dziewonski 1989, see Fig. 4), and for each density shell

one should consider independent path integrals. However, due to the complexity of these integrals we shall skip them here, providing a more detailed calculation in the Appendix.

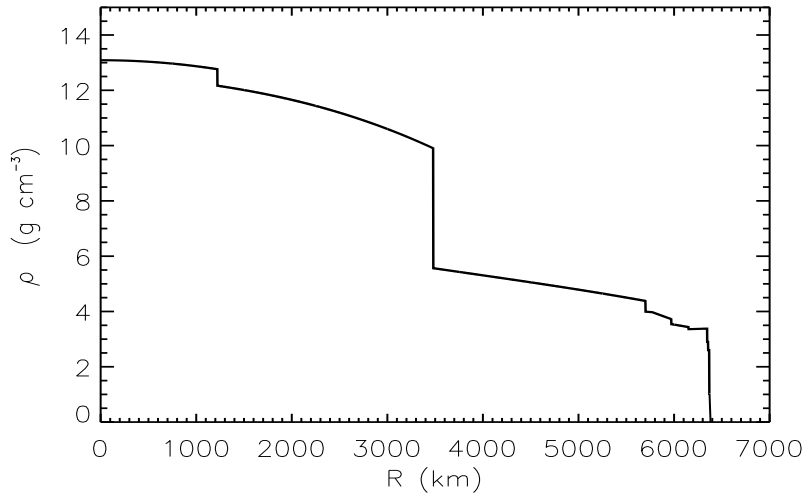


Fig. 4.— The Inner terrestrial density profile inferred from the Earth Preliminary Model.

Alternatively for each chord described by a neutrino traversing the Earth, one may introduce the column depth  $D(\theta)$  defined as  $\int \rho(r)dl$ , the integral of the density  $\rho(r)$  of the Earth along the neutrino path at a given angle  $\theta$ . The angle  $\theta$  is included between the neutrino arrival direction and the tangent plane to the earth at the observer location (see Fig. 3) ( $\theta = 0^\circ$  corresponds to a beam of neutrinos tangential to the earth’s surface) and it is complementary to the nadir angle at the same location. The function  $D(\theta)$  is displayed in Fig. 5.

To calculate the effective volume we assume that the neutrino traversing the Earth is transformed in a tau lepton at a depth  $x$ , after having travelled for a distance  $D(\theta) - x$ . The probability for the neutrino with energy  $E_\nu$  to survive until that distance is  $e^{-(D(\theta)-x)/L_\nu}$ , while the probability for the tau to exit the Earth is  $e^{-x/l_\tau}$ . On the other hand, as we

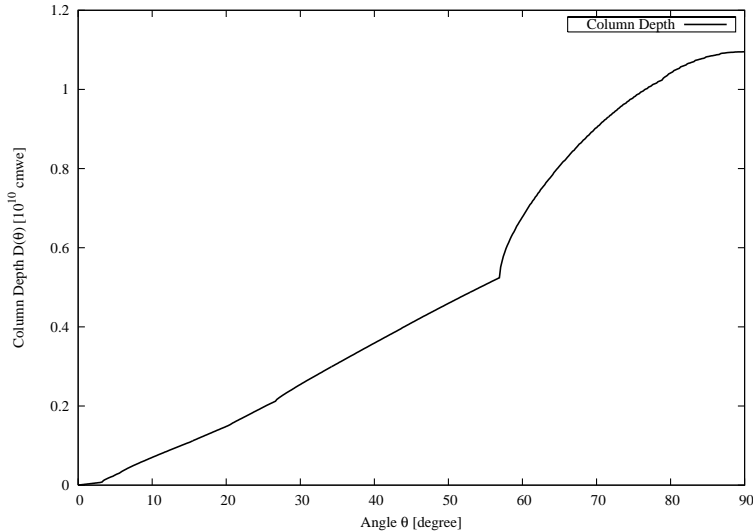


Fig. 5.— Column depth as a function of the incoming angle having assumed the multi-layers structure given by the Earth Preliminary Model.

will show in the next section, the probability for the outgoing  $\tau$  to emerge from the Earth keeping its primary energy  $E_{\tau_i}$  is  $e^{-x/L_{\tau(\beta)}}$ . By the interaction length  $L_{\nu}$  we mean the characteristic length for neutrino interaction; as we know its value may be associated to the inverse of the total cross-section  $\sigma_{Tot} = \sigma_{CC} + \sigma_{NC}$ , including both charged and neutral current interactions. It is possible to show that using the  $\sigma_{CC}$  in the  $e^{-(D(\theta)-x)/L_{\nu}}$  factor includes most of the  $\nu_{\tau}$  regeneration along the neutrino trajectory making simpler the mathematical approach. Indeed the use of the total cross-section in the opacity factor above must be corrected by the multi-scattering events (a neutral current interaction first followed by a charged current one later); these additional *relay* events (“regenerated taus”) are summarized by the less suppressing  $\sigma_{CC}$  factor in the  $e^{-(D(\theta)-x)/L_{\nu CC}}$  opacity term. The only difference between the real case and our very accurate approximation is that we are neglecting a marginal energy degradation (by a factor 0.8) for only those “regenerated taus” which experienced a previous neutral current scattering. At energy below  $10^{17}$  eV there is also a minor  $\nu_{\tau}$  regeneration (absent in  $\mu$  or  $e$  case) that may be neglected because of its

marginal role in the range of energy ( $\gg 10^{17}$  eV) we are interested in.

The effective volume is given by

$$\frac{V_{Tot}(E_\nu)}{A} = \int_0^{\frac{\pi}{2}} \int_0^{D(\theta)} e^{-\frac{D(\theta)-x}{L_{\nu CC}(E_\nu)}} e^{-\frac{x}{l_\tau(E_\tau)}} \sin \theta \cos \theta d\theta dx \quad (1)$$

Under the assumption that the  $x$  depth is independent of  $L_\nu$  and  $l_\tau$ , the above integral becomes:

$$\frac{V_{Tot}(E_\nu)}{A} = \left( \frac{l_\tau}{1 - \frac{l_\tau}{L_\nu}} \right) \int_0^{\frac{\pi}{2}} \left( e^{-\frac{D(\theta)}{L_{\nu CC}(E_\nu)}} - e^{-\frac{D(\theta)}{l_\tau(E_\tau)}} \right) \sin \theta \cos \theta d\theta \quad (2)$$

Given that  $e^{-\frac{D(\theta)}{l_\tau}} \ll e^{-\frac{D(\theta)}{L_{\nu CC}}}$ , the second exponential in the integral may be neglected and the relation can be rewritten as

$$\frac{V_{Tot}(E_\tau)}{A} = \left( \frac{l_\tau(E_\tau)}{1 - \frac{l_\tau(E_\tau)}{L_\nu(\eta E_\tau)}} \right) \int_0^{\frac{\pi}{2}} e^{-\frac{D(\theta)}{L_{\nu CC}(\eta E_\tau)}} \sin \theta \cos \theta d\theta \quad (3)$$

where the energy of the neutrino  $E_\nu$  has been expressed as a function of  $E_\tau$  via the introduction of the parameter  $\eta = E_\nu/E_{\tau_f}$ , the fraction of energy transferred from the neutrino to the lepton. At energies greater than  $10^{15}$  eV, when all mechanisms of energy loss are neglected,  $\eta = E_\nu/E_{\tau_f} = E_\nu/E_{\tau_i} \simeq 1.2$ , meaning that the 80 % of the energy of the incoming neutrino is transferred to the newly born  $\tau$  after the  $\nu - N$  scattering (Gandhi 1996, 1998).

When the energy losses are taken into account, the final  $\tau$  energy  $E_{\tau_f}$  is a fraction of the one at its birth,  $E_{\tau_i}$ . Their ratio  $x_i = E_{\tau_f}/E_{\tau_i}$  is related to  $\eta$  by the following expression

$$\eta(E_{\tau_f}) = \frac{E_\nu}{E_{\tau_f}} = \frac{E_\nu}{E_{\tau_i}} \frac{E_{\tau_i}}{E_{\tau_f}} \simeq \frac{1.2}{x_i(E_{\tau_f})}.$$

Once the effective volume is found, we introduce an effective mass defined as

$$\frac{M_{Tot}}{A} = \rho_{out} \frac{V_{Tot}}{A} \quad (4)$$

where  $\rho_{out}$  is the density of the outer layer of the Earth crust:  $\rho_{out} = 1.02$  (water) and 2.65 (rock). Before showing the effective Volume and Mass in Figure 9 for different densities we discuss the  $\tau$  lepton energy losses needed to estimate the above formula.

#### 4.2. Neutrino and Tau Interactions and Energy losses: the beta function

Ultrahigh-energy tau neutrinos may be detected by observing tau air showers originated in the  $\nu-N$  interactions as a neutrino beam crosses the Earth. The tau lepton energy is the only observable quantity we can measure, therefore we have to determine the relation between the energy of the primary neutrino and of the outgoing lepton  $\tau$ ,  $E_{\nu_i} = E(E_{\tau_f})$ . Moreover, one has to consider that  $\tau$  leptons traveling across the Earth lose energy while interacting with the nucleons. At low energies the relation between  $E_\nu$  and  $E_\tau$  is easy to define, and it may be approximated as  $E_{\tau_i} = (1 - y)E_\nu$  where  $y \sim 0.2$  is the fractional energy transferred to the nucleus. The elasticity parameters are different for the  $\nu$  and  $\bar{\nu}$ . While at low energy they differ by nearly a factor 2, at highest energy  $y$  converges to the same 0.8 limit for both neutrinos. We use their average value in our analysis.

Increasing the energy, different mechanisms suppress the lepton's propagation: first ionization, then bremsstrahlung, pair production and (at  $E > 10^8 GeV$ ) photo-nuclear reactions dominate our calculation of the emerging final lepton energy  $E_{\tau_f}$ . The energy losses are described by the equation

$$-\frac{dE}{dX} = \alpha + \beta E \quad (5)$$

where  $\alpha$ , the ionization energy loss, is negligible at energies above several hundreds GeV and  $\beta = \sum_i \beta_i$  is the sum of the remaining three mechanisms, each one denoted by the index  $i$ . For tau leptons the photonuclear and pair production processes are more important compared to bremsstrahlung (Dutta et al. 2001), but above  $10^5$  GeV the photonuclear interactions become the most efficient mechanism of energy loss. The  $\beta$  value is weakly dependent on the energy and for small slant depth  $dX$  it may be assumed as constant. Thus, the final energy of the tau becomes  $E_{\tau_f} = E_{\tau_i} e^{-\beta(E_{\tau_i})dX}$ , where  $(\rho\beta^{-1})$  defines a scale-length where the energy of the leptons is not severely suppressed. Fig. 6 displays the  $\beta$  dependence on the tau energy for leptons propagating through rock and water, including all the three components (bremsstrahlung, pair production and photonuclear interactions) whose expression has been derived by Dutta et al. (2001) for the rock and by Jones et al. (2004) for the water. Here both functions have been extrapolated to higher energies.

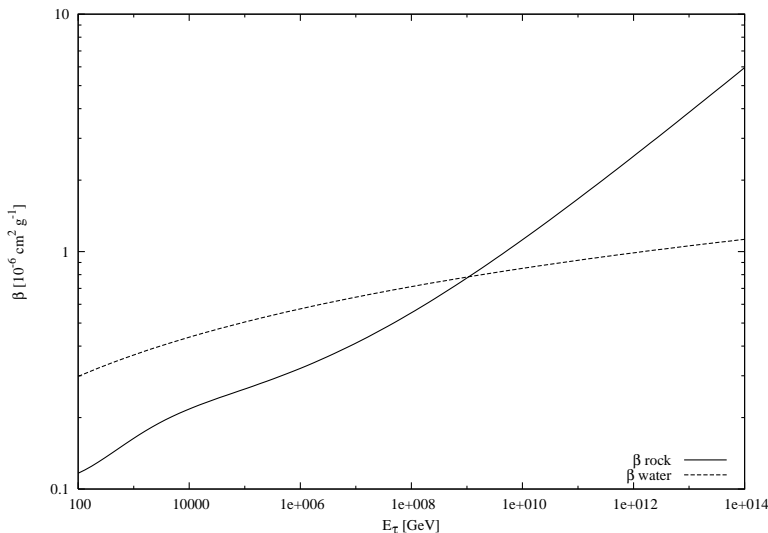


Fig. 6.— Beta energy values in water ( $\rho = 1$ ) and rock ( $\rho = 2.65$ )

In Fig. 8 we show the tau interaction length for different matter densities. When energy losses are negligible the tau range is given by the tau decay length  $R_{\tau}$ . Including the energy losses the tau propagation is suppressed compared to the free decay length.

The  $\tau$  interaction length -  $l_\tau$  - for escaping leptons from the Earth has been derived with a convenient approximation of the solution of the following pair of transcendent equations (see Fargion 2002a for a more detailed description)

$$\frac{\ln(1/x_i)}{\rho_r[\beta_{0\tau} + \beta_{1\tau} \ln(E_{\tau_i}/E_{0\tau})]} = 492x_i \frac{E_{\tau_i}}{E_{0\tau}} \quad (6)$$

$$\frac{\ln(1/x_i)}{\rho_r[\beta_{0\tau} + \beta_{1\tau} \ln(E_{\tau_i}x_i/E_{0\tau})]} = 492x_i \frac{E_{\tau_i}}{E_{0\tau}} \quad (7)$$

where  $x_i = (E_{\tau_f}/E_{\tau_i})$ ,  $E_{0\tau} = 10^{14}$  eV, 492 is the tau length in cm at this energy, and  $\beta_{0\tau}$  contains comparably constant terms from pair production and photo-nuclear interactions, while  $\beta_{1\tau}$  is mainly due to photo-nuclear effects.

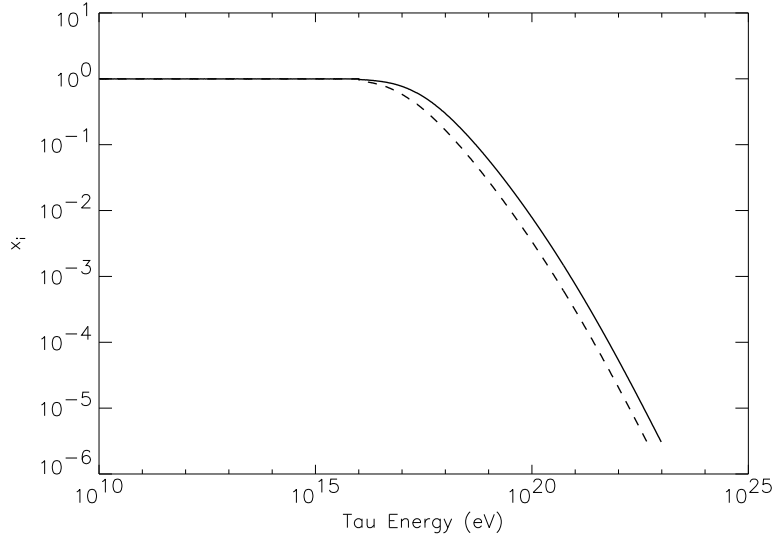


Fig. 7.— The ratio between the final and initial  $\tau$  energy ratio in water (solid line) and in rock.

For instance we have used as a convenient expression for the water  $\beta_{0\tau} = 2.3 \cdot 10^{-7}$  cm<sup>2</sup>



$\text{g}^{-1}$  and  $\beta_{1\tau} = 4.5 \cdot 10^{-8} \text{ cm}^2 \text{ g}^{-1}$  (see Fargion 2002a). However in this paper we use the exact behaviour of  $\beta$  as a function of  $E_\tau$ , as it is displayed in Fig. 8 containing all the terms contributing to the energy losses respectively for water and rock. The  $\tau$  interaction length is then given by

$$l_\tau = 492 x_i \frac{E_{\tau i}}{E_{0\tau}} \text{ cm} \quad (8)$$

where the  $x_i$ , displayed in Fig. 7 as a function of the outgoing  $\tau$  energy, is the average value found at any energy by the set of two independent transcendental equations above.

At highest energies, above  $10^{10}$  GeV weak interactions play a role in the energy losses of the  $\tau$ . The interaction length of the charged-current  $\tau N$  process is shorter than the tau decay length above  $10^{10}$  GeV but already the energy losses length-scale (mainly due to nuclear losses ) suppress the tau propagation at earlier high energies. In Fig. 8 (left-hand side) this interaction length is indicated as  $L_{\nu CC}$ , since one can show that the cross section of the electro-weak reaction  $\tau - N$  is equivalent to the one of the  $\nu - N$  scattering (Fargion 2002a). These three processes combine into the curve  $l_\tau$  shown in Fig. 8 that we have calculated for both water and rock.

Finally, in the righthand side of Fig. 8 we compare the value of  $l_\tau$  with the scale-length defined by  $L_{\tau(\beta)}$ , that we will use for our calculation of the inner effective volume for tau surviving with most primary energy. This interaction length is defined as

$$L_{\tau(\beta)} = \left( \beta \rho + \frac{1}{L_{\nu CC}} + \frac{1}{R_\tau} \right)^{-1} \quad (9)$$

Again it is displayed for a  $\tau$  propagating through water (dash line) and rock (dotted line) and it is compared with  $l_\tau$ . Compared to  $l_\tau$ , the interaction  $L_{\tau\beta}$  is shorter at energies greater than few times  $10^{17}$  eV, therefore it defines a thinner effective volume. Within

such interaction volume the outgoing  $\tau$  preserves most of the initial energy determining a harder tau air-shower spectrum. This procedure gives results equivalent to those of Monte-Carlo predictions which we did verify but are not displayed here.

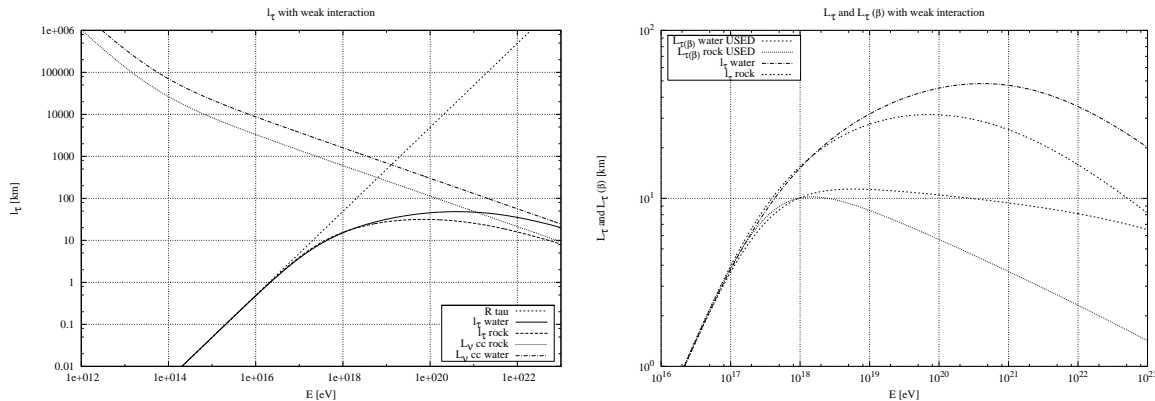


Fig. 8.— **left**) Lepton  $\tau$  interaction Lengths for different matter densities:  $R_\tau = c \cdot \tau_\tau \cdot \gamma_\tau$  is the free  $\tau$  range (dashed line),  $l_\tau$  is the  $\tau$  propagation length in water (solid line) and rock (thick dashed line), including all known interactions and energy losses.  $L_{\nu CC}$  is the  $\tau$  propagation length due to electro-weak interactions with nucleons, ( $\tau - N$ ), and it is equivalent to that of the  $\nu - N$  scattering (Fargion 2002a). Again this length is displayed for both water (dashed-dotted line) and rock (dotted line) densities. **right**) Comparison between  $L_{\tau(\beta)}$  and  $l_\tau$  for rock and water. The latter curves ( $l_\tau$ ) are identical (but in different scale) to those shown on the left-hand side. As one can see from the picture,  $L_{\tau(\beta)}$  is shorter than  $l_\tau$  at energies above  $10^{17}$  eV, thus it corresponds to a smaller effective volume where  $\tau$ 's are produced while keeping most of the primary neutrino energy. The energy label on the x axis refers to the newly born tau.

### 4.3. Final $\tau$ skin effective volume in different detectors

Having derived the relation between  $E_{\nu_i}$  and  $E_{\tau_f}$ , and having defined a length scale for the tau energy losses, we can calculate the  $\tau$  skin volume as a function of the  $\nu$  as well as  $\tau$

energy. We remind to the reader that  $V_{eff}$  is the effective volume where Ultra High Energy neutrinos interactions within the Earth lead to UHE Taus. In this section we introduce the complete calculation and we show the plots of the corresponding effective volume and mass for the Earth preliminary model. In Fig 9 we are showing the effective volume  $V_{eff}(E_{\nu_i})$  and its consequent mass  $M_{eff}(E_{\nu_i})$  for a detection acceptance of  $A = 1 \text{ km}^2$ , considering the simplest case where we include all the  $\tau$  events regardless of the exact  $\tau$  final energy and neglecting the  $\tau$  air-shower occurrence.

At  $10^{19}$  eV we find an effective Volume  $V_{eff} = 2 \cdot 10^{-2} \text{ km}^3$  and a mass  $M_{eff} = 2 \cdot 10^{-2} \text{ km}^3$  (water equivalent) assuming an outer layer of the Earth made of water ( $\rho = 1.02$ ). For the rock instead we obtain  $V_{eff} = 1.86 \cdot 10^{-2} \text{ km}^3$ , and  $M_{eff} = 4.95 \cdot 10^{-2} \text{ Km}^3$  (water equivalent). This simple result states the dominant role of UPTAUs and HORTAUs volume and masses compared to the downward induced neutrino events in air:  $V_{air} = 10^{-2} \text{ km}^3$ ,  $M_{eff} = 10^{-2} \text{ Km}^3$  (water equivalent) in the wide energy window  $10^{16} \text{ eV} < E_{\nu_i} < 10^{20} \text{ eV}$  almost un-affected by any atmospheric neutrino background.

We first present the calculation of effective mass and volume in two cases: first for a generic detector with an acceptance of one km square unit area, then we present the same calculation for the characteristics of the EUSO experiment. Finally we compare EUSO with the Auger observatory.

The expression of the effective volume in the most general case, using the Earth preliminary model is given by

$$\frac{V_{Tot}(E_\tau)}{A} = \left( \frac{L_{\tau(\beta)}(E_\tau)}{1 - \frac{L_{\tau(\beta)}(E_\tau)}{L_{\nu_{CC}}(\eta E_\tau)}} \right) \int_0^{\frac{\pi}{2}} e^{-\frac{D(\theta)}{L_{\nu_{CC}}(\eta E_\tau)}} \sin \theta \cos \theta d\theta \quad (10)$$

where  $L_{\tau\beta}$  is defined by Eq. 9. This interaction length (shorter than  $l_\tau$ ) guarantees a high energy outcoming  $\tau$  even if from a thinner Earth crust.

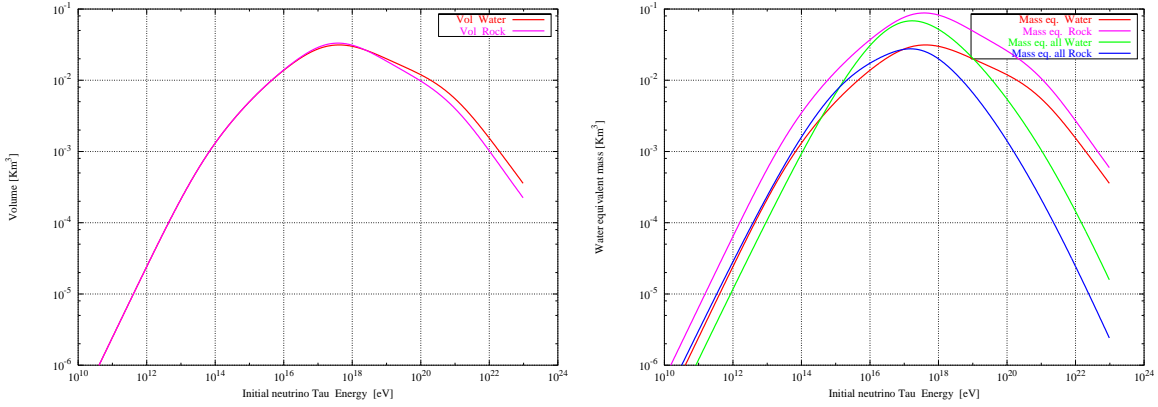


Fig. 9.— **left)** The effective Volume for UPTAUs and HORTAUs for a detector acceptance of  $1 \text{ km}^2$  having neglected the role of the atmospheric layer in the development of the tau air shower. We have chosen  $\eta = 1.2$ , implying that the 80 % of the initial neutrino energy has been transferred to the newly born  $\tau$ . The volume has been estimated as in Eq. 3 using  $l_\tau$  as interaction length. **right)** The corresponding effective Mass for UPTAUs and HORTAUs per  $\text{km}^2$  (see Eq. 4) with the same approximations used for the calculation of the volume. The two additional curves represent a simplified model of the Earth treated as an unique homogeneous sphere of water ( $\rho = 1$ ) or of rock ( $\rho = 2.65$ ). The horizontal line at  $M = 10^{-2} \text{ km}^3$  corresponds to the air mass above the same  $\text{km}^2$  area. Note that the masses for an Earth made entirely of water or rock has been obtained under the assumption of a finite thickness for the terrestrial atmosphere (an horizontal extension of 600 km). The same constraint will be applied to the final calculation of the effective volume and mass.

The terrestrial cord,  $D(\theta)$ , is responsible for the  $\nu_\tau$  opacity, and  $L_\nu$  is the interaction length for the incoming neutrino in a water equivalent density, where  $L_{\nu CC} = (\sigma_{CC} n)^{-1}$ . It should be kept in mind that both  $L_\nu$  and  $D(\theta)$ , the water equivalent cord, depend on the number density  $n$  (and the relative matter density  $\rho_r$ ). We remind that the total neutrino cross section  $\sigma_\nu$  consists of two main component, the charged current and neutral current terms, but the  $\tau$  production depends only on the dominant charged current whose role will appear later in the event rate number estimate. The interaction lengths  $L_{\tau\beta}$ ,  $L_{\nu CC}$ , depends on the energy, but one should be careful on the energy meaning. Here we consider an incoming neutrino with energy  $E_{\nu_i}$ , a prompt  $\tau$  with an energy  $E_{\tau_i}$  at its birth place, and a final outgoing  $\tau$  escaping from the Earth with energy  $E_{\tau_f}$ , after some energy losses inside the crust. The final  $\tau$  shower energy, which is the only observable quantity, is nearly corresponding to the latter value  $E_{\tau_f}$  because of the negligible  $\tau$  energy losses in air. However we must be able to infer  $E_{\tau_i}$  and the primary neutrino energy,  $E_\nu$ , to perform our calculation. The effective volume and masses resulting from Eq. 10 are displayed in Fig. 10.

However one has to take into account the presence of the Earth atmosphere which implies a further suppression of the effective volume especially at high energies. Therefore Eq. 10 becomes

$$\frac{V_{Tot}(E_\tau)}{A} = \left(1 - e^{-\frac{L_0}{c\tau\gamma\tau}}\right) \left(\frac{L_{\tau(\beta)}(E_\tau)}{1 - \frac{L_{\tau(\beta)}(E_\tau)}{L_{\nu CC}(\eta E_\tau)}}\right) \int_0^{\frac{\pi}{2}} e^{-\frac{D(\theta)}{L_{\nu CC}(\eta E_\tau)}} \sin\theta \cos\theta d\theta \quad (11)$$

where the first term outside the integral guarantees that the relativistic  $\tau$  length will never exceed the longest inclined path through the Earth's atmosphere ( $L_o \simeq 600 \text{ Km}$ ) corresponding to a characteristic height  $h_1 \simeq 23 \text{ Km}$  (Fargion 2001b, 2002a).

The effective volume and mass obtained in this case are shown in Fig. 11 for an acceptance of  $1 \text{ km}^2$  unit area. Even if the Effective Volumes and Masses are now reduced

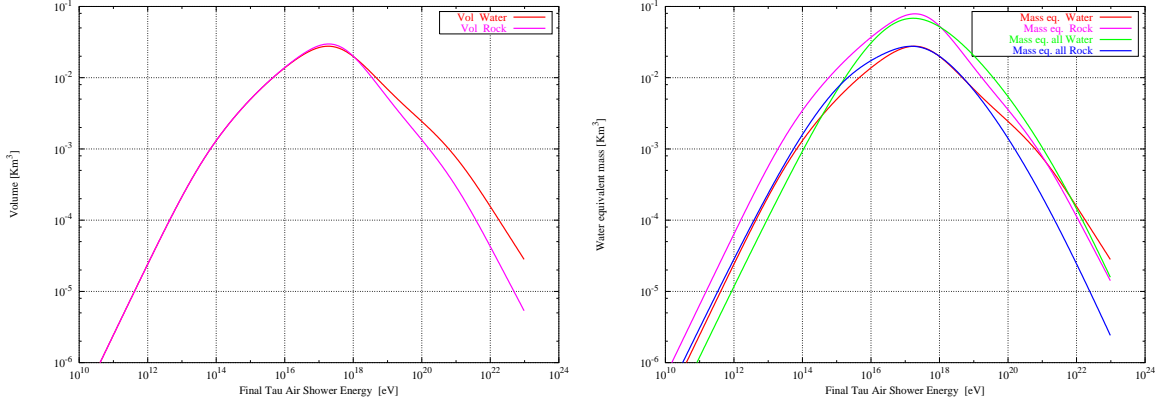


Fig. 10.— **left)** Effective Volume for UPTAUs and HORTAUs per km<sup>2</sup> unit area neglecting the finite extension of the horizontal atmospheric layer. Here the calculation has been performed using the most restrictive interaction length  $L_{\tau(\beta)}$ . Therefore on the x axis we have plotted the final energy of the tau lepton, rather than the initial neutrino energy as in Fig. 9. Again the two curves correspond to an outer layer made of water (solid line) and an outer layer made of rock (dotted line). **right)** Effective Mass for UPTAUs and HORTAUs per km<sup>2</sup> unit area derived under the same assumptions. As in Fig. 9 the curves obtained are compared with a simplified model of the Earth, considered as an homogeneous sphere of water (dashed line) and rock (big dotted line). Again, note that in these cases the masses have been obtained under the constraint of a finite extension of the terrestrial atmosphere (an horizontal length of 600 km).

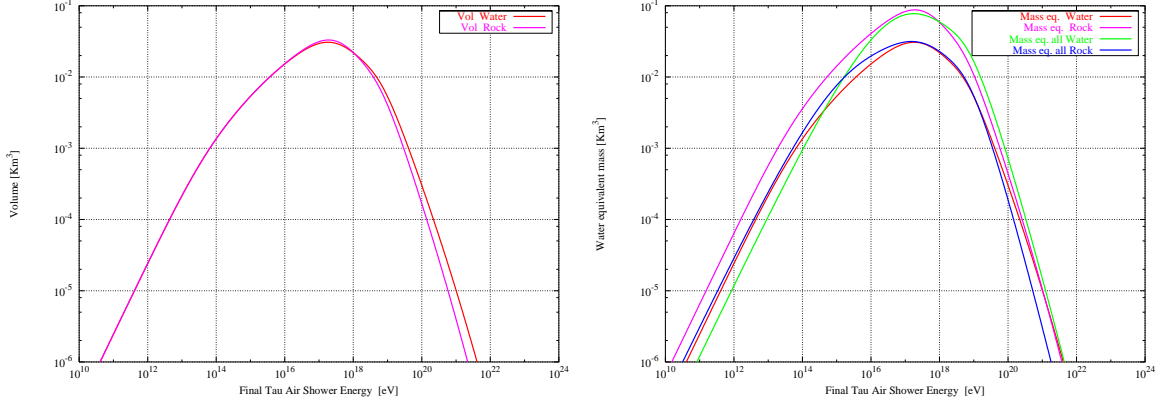


Fig. 11.— **left)** Effective Volume for UPTAUs and HORTAUs per km square unit area including the suppression factor due to the finite extension of the horizontal atmospheric layer. Again, the calculation has been performed using the most restrictive interaction length  $L_{\tau(\beta)}$  and the volume is expressed as a function of the final tau energy. **right)** The corresponding effective Mass for UPTAUs and HORTAUs for km square unit area.

these values still exceeds those of the atmospheric layer above the same  $km^2$  area. Moreover it should be emphasized that the detection of downward neutrino induced air-shower is affected by different experimental problems. Most of the vertical events cross a too small slant depth, they can not develop a full air-shower and their signature is hidden in the UHECR downward background. Therefore HORTAUs are still the most relevant tracers of UHE  $\tau$  neutrinos in the range of energy between  $10^{16}$  eV and  $10^{20}$  eV.

Among current and future neutrino detectors we would like to narrow our analysis down to two different projects capable of indirectly searching Tau Air-Showers: the ground-based arrays of scintillator/photomultipliers which constitutes the Auger project, and the space observatory EUSO, whose characteristics have been described in section §3. EUSO may detect HORTAUs (Horizontal Tau Air-Showers) originated within a very wide terrestrial skin volume around its field of view (FOV), corresponding to a few hundred kilometer radius wider area. A schematic picture its field of view and the kind of air-showers it may

be able to observe is shown in Fig. 12.

After having derived the effective volume and mass for a 1 km<sup>2</sup> unit area detector, we finally show in Fig. 13 the Effective mass for EUSO. Note that the earliest prediction for a simplified Earth model considered as an homogeneous sphere of water and rock in the energy range 10<sup>15</sup> – 10<sup>19</sup> eV are not too different from our last result (Fargion 2002b), even though as it appears from the figure, the role of rock and water has now been inverted. Such a result has not been noticed before (Fargion 2002b, 2002c; BG03). The remarkable huge mass (either for water and rock) 7.8 · 10<sup>2</sup> km<sup>3</sup> and 1.6 · 10<sup>3</sup> water equivalent km<sup>3</sup> makes EUSO (even with 10% duty cycle) the widest neutrino telescope in Neutrino Astronomy. Other concurrent experiment (SALSA, ANITA and FORTE) are mainly neutrino collectors unable to follow their exact arrival direction.

### 5. Event Rate for GZK neutrinos with EUSO

The consequent event rate for incoming neutrino fluxes may be easily derived by:

$$\frac{dN_{ev}}{d\Omega dt} = \left( \int \frac{dN_\nu}{dE_\nu d\Omega dAdt} \sigma_{N\nu}(E) dE \right) n \rho_r V_{Tot} \quad (12)$$

If the cross section is slowly varying with the energy (as it is in the  $\nu N$  reaction), the integral reduces to

$$\frac{dN_{ev}}{d\Omega dt} = \frac{dN_\nu E_\nu}{dE_\nu d\Omega dAdt} \sigma_{N\nu} n \rho_r V_{Tot} = \frac{\phi_\nu}{L_{\nu CC}} \rho_r V_{Tot} \quad (13)$$

where  $(\sigma_{N\nu} n)^{-1} = L_{\nu CC}$  and  $\phi_\nu = \frac{dN_\nu E_\nu}{dE_\nu d\Omega dAdt}$ , and  $\rho_r$  is the density of the layer relative to the water. As it has been mentioned in the previous section we have neglected the  $\nu_\tau - N$  scattering via the neutral current channel. This process causes a  $\nu_\tau$  regeneration through a



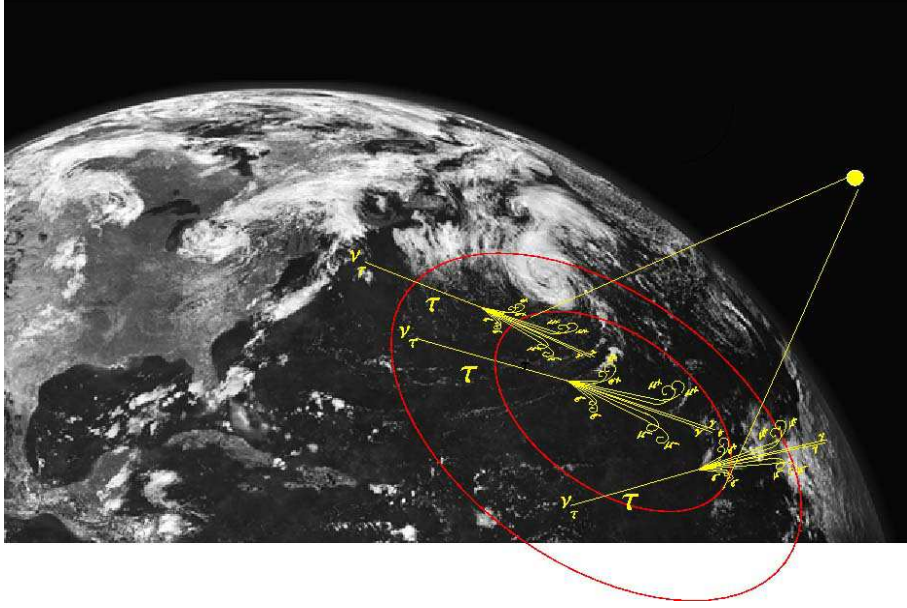


Fig. 12.— A schematic figure showing the field of view (FOV) of EUSO where  $\tau$  air-shower are taking place. We note that the EUSO threshold energy above  $\sim 10^{19}$  eV implies  $\tau$  tracks longer than 500 km, consequently only UHE neutrino interacting within a much wider terrestrial crust (700 – 900 km radius rings) might produce HORTAUs observable within the telescope’s FOV. The correspondence between the outcoming  $\tau$  along the wide ring (producing the HORTAUs pointing to the EUSO FOV) and consequent HORTAUs observed within the same FOV, guarantees the equivalence between the effective volumes defined by these two different regions. There are three main groups of HORTAUs: the showers totally included in the FOV, and those that are partially contained in the FOV (both incoming and outgoing); the latter will exceed the fully contained ones. The HORTAUs should extend for a few hundred km in horizontal and reach tens of kilometers in altitude. Such showers should be opened by geo-magnetic forces into thin, fan-shaped, charged and neutral jet tails, mainly observable as forked and diffused Cherenkov lights. Their characteristic opening is ruled by the local geo-magnetic field strength and directionality.

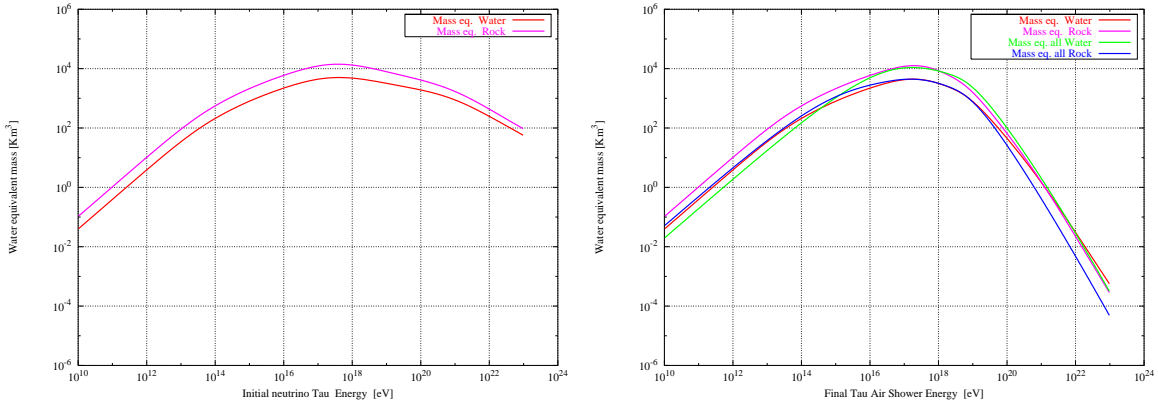


Fig. 13.— **left)** Effective Mass for UPTAUs and HORTAUs for EUSO as a function of the incoming neutrino energy, calculated with the interaction length  $l_\tau$ . Here we have neglected the finite horizontal extension of Earth’s atmosphere. The water mass-volume at  $E_\nu = 10^{19}$  eV, is  $3.2 \cdot 10^3 \text{ km}^3$ , while for the rock the mass-volume is  $7.9 \cdot 10^3 \text{ km}^3$ . **right)** Effective Mass for UPTAUs and HORTAUs for EUSO with  $L_{\tau(\beta)}$ , considering the finite horizontal extension of Earth’s atmosphere. The water mass-volume is  $7.8 \cdot 10^2 \text{ km}^3$ , while for the rock the volume is  $5.9 \cdot 10^2 \text{ km}^3$ . The corresponding mass is nearly  $1.6 \cdot 10^3$  water equivalent  $\text{km}^3$ .

marginal energy degradation by a factor  $(1 - y) \simeq 0.8$  where  $y$  is the inelasticity parameter (Gandhi et al. 1995, 1998). Although this term may be responsible for a sequence of  $\nu_\tau$  regeneration, its contribution to the number of events is mainly taken into account by the use of the charged current cross section (and not by the additional neutral current contribute).

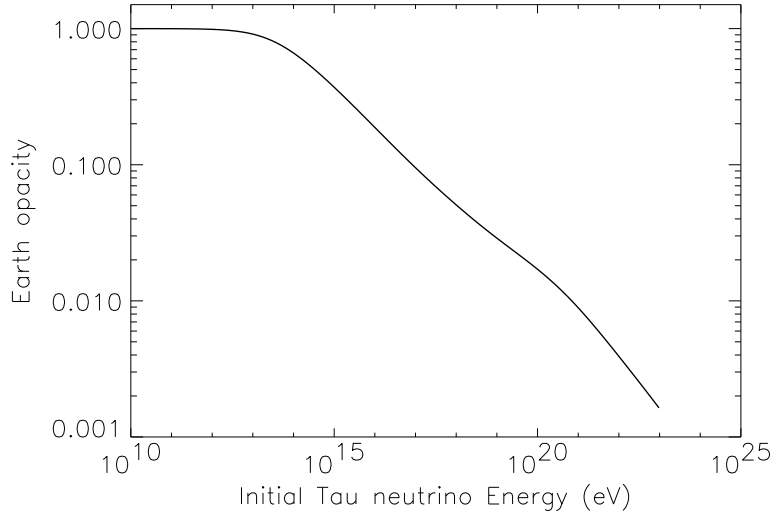


Fig. 14.— The Earth opacity to upward neutrinos as a function of the initial  $\nu_\tau$  energy.

After having introduced the effective volume we can estimate the outcoming event number rate for EUSO for any given neutrino flux. In particular this general expression will be displayed assuming a minimum GZK neutrino flux  $\phi_\nu \simeq \phi_{UHECR} \simeq 5 \cdot 10^{-18} \text{cm}^{-2} \text{s}^{-1} \text{sr}^{-1}$  comparable to the observed UHECR one at the same energy ( $E_\nu = E_{UHECR} \simeq 10^{19} \text{eV}$ ). The assumption on the flux may be changed at will and the event number will scale linearly according to the model.

However, the initial incoming  $\nu$  flux  $\phi_\nu = \frac{dN_\nu E_\nu}{dE_\nu d\Omega dA dt}$  is suppressed when neutrinos cross the Earth by a shadow factor

$$S = \int_0^{\pi/2} e^{-\frac{D(\theta)}{L_{\nu CC}}} \cos\theta d\theta$$

shown in Fig. 14. This function defines the ratio between the final outgoing upward neutrinos,  $\phi_{\nu_f}$  and the initial downward  $\phi_{\nu_i}$ ,  $S(E_{\nu_i}) = \phi_{\nu_f}/\phi_{\nu_i}$ .

In Fig. 15 we show the expected number of event per  $\text{km}^2$  to more easily compare our results with those of other authors. The results have been obtained for two different scenarios. On the left-hand side we display the number of events having neglected the presence of the atmospheric layer, with the choice of  $l_\tau$  as interaction length. Under this assumption we calculate the number of events as a function of the energy of the incoming neutrino. On the right-hand side we have included the Earth's atmosphere and we have used  $L_{\tau(\beta)}$ , thus we may express the results as a function of the final  $\tau$  lepton energy. Both scenarios have been calculated with two incoming neutrino fluxes, whose power law spectrum is proportional to  $E^{-2}$  (which approximates at highest energies the GZK flux) and  $E^{-1}$  (that mimics the Z-burst flux) respectively. In general one may imagine a power law  $E^{-\alpha}$ ,  $0 < \alpha < 1$  within the two extreme laws above. These incoming neutrino fluxes are also shown in Fig. 15, as well as the final neutrino fluxes  $\phi_{\nu_f} = S(E_{\nu_i})\phi_{\nu_i}$  for both models. One has to bear in mind that the final number of events for UPTAUs-HORTAUs is determined by the  $V_{eff}$ ,  $M_{eff}$  functions (Eqs. 1 - 4) which already take into account the Earth opacity to neutrinos with the  $\nu$  interaction length  $L_{\nu CC}$ . Therefore  $N_{ev} \propto \phi_{\nu_i}$  rather than  $N_{ev} \propto \phi_{\nu_f}$ .

At  $E^{19}$  eV in the more restrictive approximation we obtain the following number of events for an area  $\text{km}^2$  and in one year data collection :

$$N_{ev}^{water} = 2.55 \cdot 10^{-4} (\phi_\nu E_\nu / 50 \text{eV cm}^{-2} \text{s}^{-1} \text{sr}^{-1}) \quad N_{ev}^{rock} = 6.26 \cdot 10^{-4} (\phi_\nu E_\nu / 50 \text{eV cm}^{-2} \text{s}^{-1} \text{sr}^{-1})$$

As regards EUSO, the general expected event rate around the same energy range is given by:

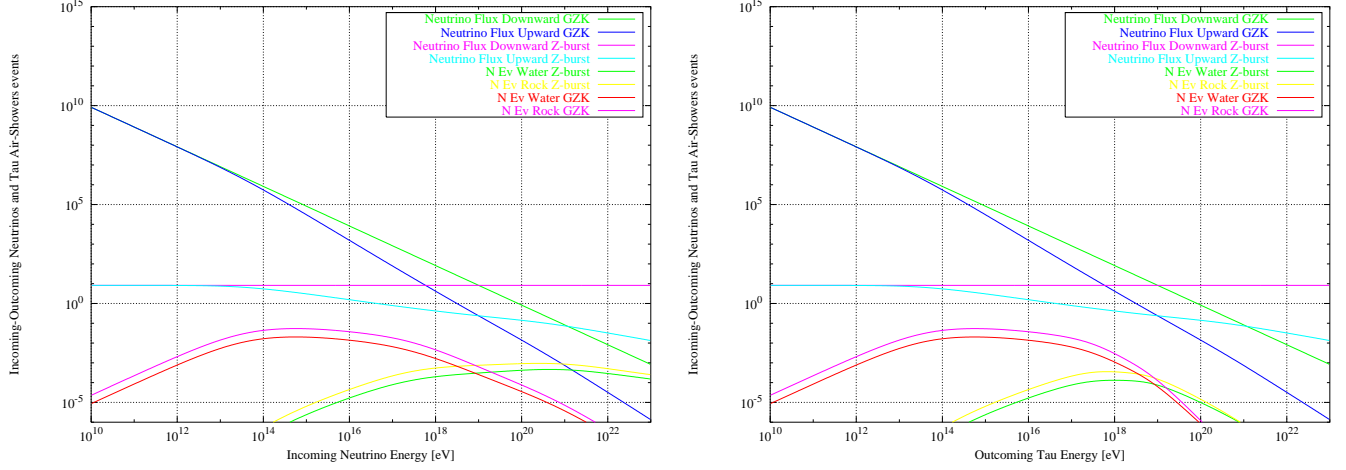


Fig. 15.— **left)** Number of HORTAUs Events per  $\text{km}^2$  and for one year data collection as a function of the incoming neutrino energy excluding the finite extension of the horizontal atmospheric layer, with a  $\tau$  lepton interaction length given by  $l_\tau$  (see Fig. 8). Here GZK and Z burst neutrino fluxes refers to the incoming upward and downward neutrino spectrum  $\propto E^{-2}$  (inclined dashed line), and  $\propto E^{-1}$  respectively (horizontal dotted-line). The outgoing neutrino curves are suppressed above energies  $10^{14}$  eV compared to the incoming  $\nu$  fluxes by the shadow factor defined in Fig. 14. For each flux the number of events is derived for an outer layer of both rock and water. At  $10^{19}$  eV we find  $N_{ev}^{water} = 2.55 \cdot 10^{-4}$  ( $\phi_\nu E_\nu / 50 \text{ eV cm}^{-2} \text{ s}^{-1} \text{ sr}^{-1}$ ) and  $N_{ev}^{rock} = 6.26 \cdot 10^{-4}$  ( $\phi_\nu E_\nu / 50 \text{ eV cm}^{-2} \text{ s}^{-1} \text{ sr}^{-1}$ ). **right)** Number of events as a function of the outgoing lepton tau for  $L_{\tau(\beta)}$ , including the finite extension of the horizontal atmospheric layer. Again the results are compared to a GZK/Z-burst neutrino flux, and they are displayed for an outer layer made of rock and water. In this case  $N_{ev}^{water} = 0.62 \cdot 10^{-4}$  ( $\phi_\nu E_\nu / 50 \text{ eV cm}^{-2} \text{ s}^{-1} \text{ sr}^{-1}$ ) and  $N_{ev}^{rock} = 1.25 \cdot 10^{-4}$  ( $\phi_\nu E_\nu / 50 \text{ eV cm}^{-2} \text{ s}^{-1} \text{ sr}^{-1}$ ).

$$N_{ev} = 5 \cdot 10^{-18} cm^{-2} s^{-1} sr^{-1} \left( \frac{V_{eff} \rho_r}{L_{\nu CC}} \right) (2\pi \eta_{Euso} \Delta t) \left( \frac{\Phi_{\nu} E_{\nu}}{50 eV cm^{-2} s^{-1} sr^{-1}} \right) \left( \frac{\eta E_{\tau}}{10^{19} eV} \right)^{-\alpha} \quad (14)$$

where  $\eta_{Euso}$  is the duty cycle fraction of EUSO,  $\eta_{Euso} \simeq 10\%$ ,  $\Delta t \simeq 3 \text{ years}$ . The consequent number of events for its area ( $1.6 \cdot 10^5 Km^2$ ) is displayed in Fig. 16 assuming both a flat power law ( $\phi_{\nu} \propto E_{\nu}^{-2}$ ) and a harder Z-Burst spectra  $\phi_{\nu} \propto E_{\nu}^{-1}$ . These spectra are very simple and nearly model independent. They also fit a Berezhinsky (1990)  $\phi_{\nu} \propto E_{\nu}^{-2}$  or a Waxman-Bachall (1997, hereafter WB97) spectra for GRB as well as the GZK flux. Here we have neglected the presence of the atmosphere above the portion of the Earth surface covered by EUSO. The event number at  $E_{\nu} = 10^{19}$  eV in such an approximation is for the EUSO area and for three years data collection:

$$N_{ev}^{water} = 12.2(\phi_{\nu} E_{\nu} / 50 eV cm^{-2} s^{-1} sr^{-1}) \quad N_{ev}^{rock} = 30(\phi_{\nu} E_{\nu} / 50 eV cm^{-2} s^{-1} sr^{-1})$$

Such number of events greatly exceed previous results by at least two orders of magnitude (Bottai et al. 2003) but are below more recent estimates (Yoshida et al. 2004).

When the Earth's atmosphere is included in the calculation of the effective volume (Eq. 11), this causes a general suppression of the event rate, especially at  $E_{\nu} > 1.2 \cdot 10^{19}$  eV. At such energies the  $\tau$  decay length exceeds the maximal thickness of the atmospheric layer ( $\simeq 600$  km), reducing the possibility of  $\tau$  shower detection with EUSO. The expected number of event in such a case is shown in Fig. 17 for both a GZK and Z-burst fluxes. As one can see from Fig. 17 we obtain

$$N_{ev}^{water} = 3.0(\phi_{\nu} E_{\nu} / 50 eV cm^{-2} s^{-1} sr^{-1}) \quad N_{ev}^{rock} = 6.0(\phi_{\nu} E_{\nu} / 50 eV cm^{-2} s^{-1} sr^{-1})$$

which is yet larger than the unity for the three years scheduled for the EUSO project. Because most of the HORTAUs would be observed partially contained (inward or outward the EUSO Field of view ) the total number of events might be doubled.

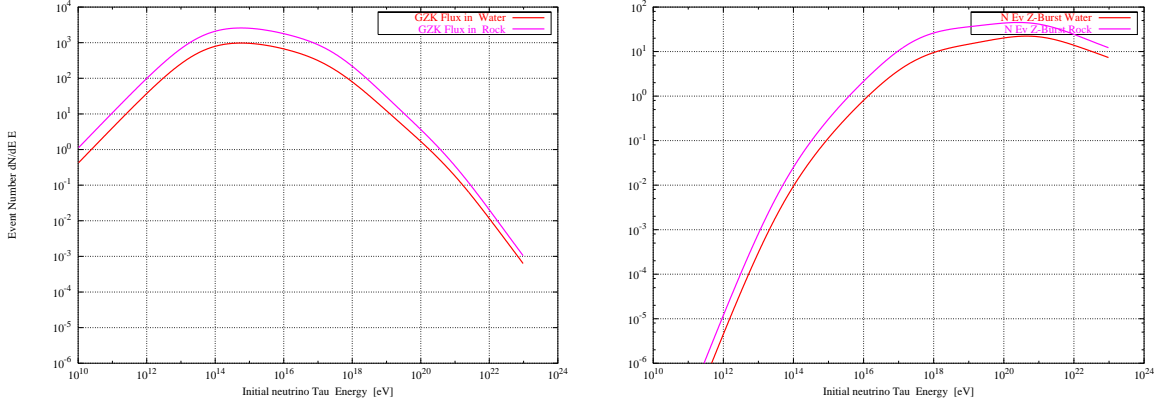


Fig. 16.— Number of EUSO Event for HORTAUs in 3 years record as a function of the incoming neutrino tau energy, having neglected the finite extension of the horizontal atmospheric layer, with  $l_\tau$  as interaction length. As above, we have used both a GZK (**left**) and a Z-burst (**right**) neutrino flux. At  $E_\nu = 10^{19}$  eV, the expected event number is 12.2 ( $\phi_\nu E_\nu/50$  eV  $\text{cm}^{-2} \text{s}^{-1} \text{sr}^{-1}$ ) for the water and 30 ( $\phi_\nu E_\nu/50$  eV  $\text{cm}^{-2} \text{s}^{-1} \text{sr}^{-1}$ ) for the rock.

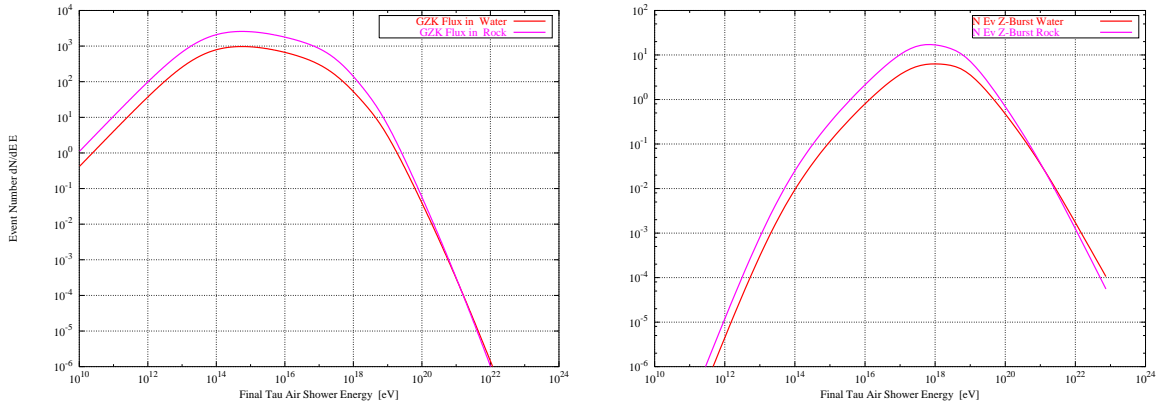


Fig. 17.— Number of EUSO Event for HORTAUs in 3 years record as a function of the outgoing lepton tau ( $L_{\tau(\beta)}$  as interaction length), including the finite extension of the horizontal atmospheric layer. At energy  $E_\tau = 10^{19}$  eV, the event number is  $N_{ev} = 3.0$  ( $\phi_\nu E_\nu/50$  eV  $\text{cm}^{-2} \text{s}^{-1} \text{sr}^{-1}$ ) for the water and  $N_{ev} = 6.0$  ( $\phi_\nu E_\nu/50$  eV  $\text{cm}^{-2} \text{s}^{-1} \text{sr}^{-1}$ ) for the rock. Again, we show the resulting number of events for two different neutrino fluxes:  $\propto E^{-2}$  GZK (**left**) and  $\propto E^{-1}$  (Z-burst **right**).

It should be kept in mind that the plots of the EUSO number of events in Fig. 16, 17 are already suppressed by a factor 0.1 due to the minimal duty cycle factor  $\eta_{EUSO}$ .

In Fig. 18 we summarize our results with and without the presence of the Earth’s atmosphere and we compare the obtained number of events with the upward and downward neutrino fluxes for a GZK and Z-burst spectrum.

It is worth noticing that the number of horizontal  $\tau$  showers observable by EUSO in three years record time is above unity at energies below  $E_\tau \simeq 10^{19} eV$ , with a peak around  $10^{18} eV$ . This is quite a remarkable result which may strengthen the case of extending the EUSO energy sensitivity below  $10^{19} eV$  by enlarging the size of the telescope. The rich Cherenkov diffused lights from HORTAUs might produce enough photons to allow a lower (than  $10^{19} eV$ ) energy threshold.

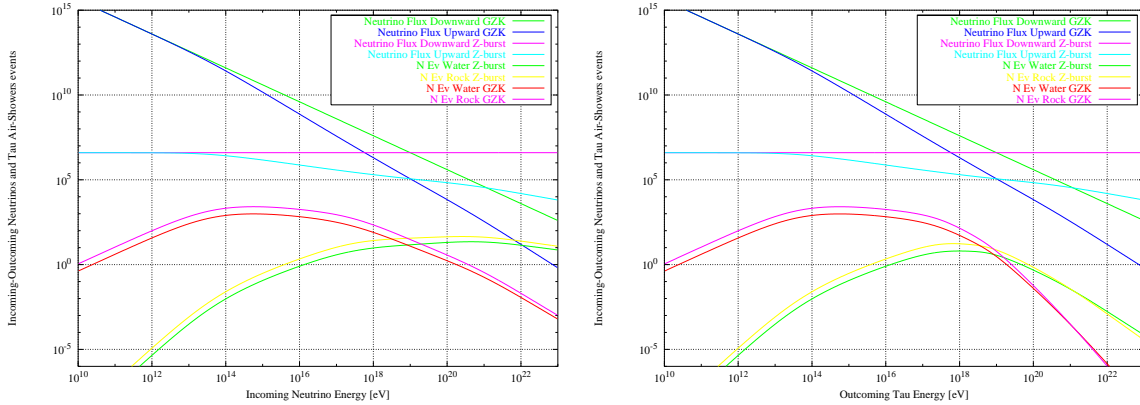


Fig. 18.— Number of EUSO Event for HORTAUs in 3 years record compared to the upward and downward neutrino flux (GZK, mostly comparable to a flux  $\propto E^{-2}$ , and Z-burst  $\propto E^{-1}$ ). The curves describing the number of events on the left and righthand side are the same as Fig. 16 (using  $l_\tau$  and neglecting the atmosphere) and Fig. 17 (using  $L_{\tau(\beta)}$  and including the atmosphere) respectively.



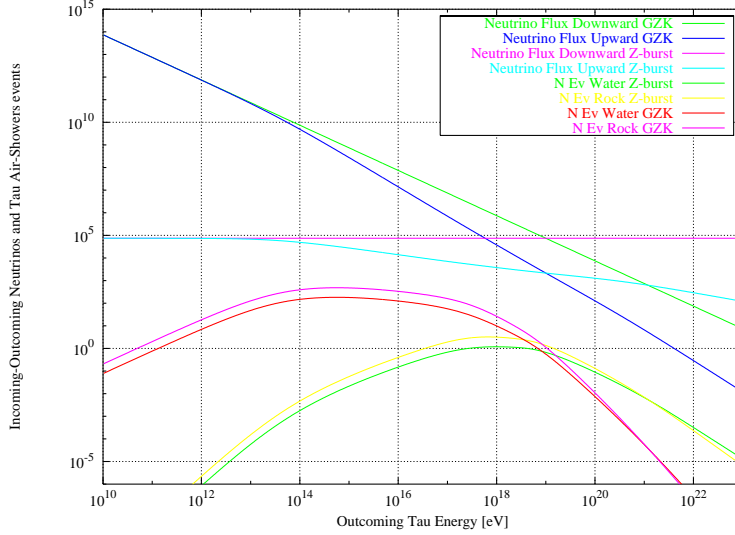


Fig. 19.— Number of Events of HORTAUs expected to be detected by Auger in 3 years record, having neglected the finite extension of the horizontal atmospheric layer. Again, we show the results for two different neutrino fluxes: GZK and Z-burst. As one can see the number of events is slightly above the unity at  $E = 10^{19}$  eV. However at energy as low as  $E = 10^{18}$  eV in GZK model the number of events increases to 26.3 for a rock layer: the most remarkable signature will be a strong azimuthal asymmetry (East-West) toward the high Andes mountain chain. The Andes shield UHECR (toward West) suppressing their horizontal flux. These horizontal showers originated in the atmosphere at hundreds of km, are muon-rich as well as poor in electron pair and gammas and are characterized by a short time of arrival. On the other hand the presence of the mountain chains at 50 – 100 km from the Auger detector will enhance by a numerical factor 2 – 6 (for each given geographical configuration) the event number respect to the East direction. These rare nearby (few or tens of km) tau air-shower will be originated by Horizontal UHE neutrinos interacting inside the Andes. These showers will have a large electron pair, and gamma component greater than the muonic one, and a dilution in the time of arrival.

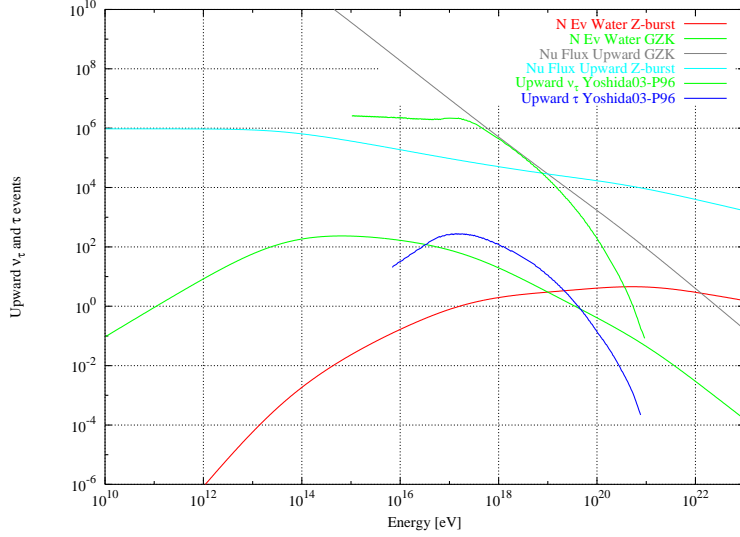


Fig. 20.— Number of EUSO Event for HORTAUs in 3 years record, having neglected the finite extension of the horizontal atmospheric layer, compared to the results of Yoshida et al. (2004). Here the assumed a lower GZK and Z-Burst like spectra ( $\phi_\nu E_\nu/10 \text{ eV cm}^{-2} \text{ s}^{-1} \text{ sr}^{-1}$ ) and we are evaluating the events assuming a water target, while Yoshida considered an almost comparable (0.9 lower density) ice mass. There is a partial disagreement: Yoshida predictions are at least a factor 2.7 at  $E = 10^{19} \text{ eV}$  and nearly an order of magnitude at  $E = 10^{18} \text{ eV}$  larger than ours. At PeVs-EeVs energies where comparison with Gandhi et al. (1998) was possible we found a general agreement. On the contrary the Bottai & Giurgula. (2003) (see their Fig.11,c) expectations are in complete disagreement with us, leading to a number of events at least two order of magnitude smaller than ours.

	$N_{ev}^{water}$ atmosphere included	$N_{ev}^{rock}$ atmosphere included	$N_{ev}^{water}$ no atmosphere	$N_{ev}^{rock}$ no atmosphere
km <sup>2</sup> (1 yr) <sup>-1</sup>	0.62·10 <sup>-4</sup>	1.25 · 10 <sup>-4</sup>	2.55 · 10 <sup>-4</sup>	6.26 · 10 <sup>-4</sup>
Auger (3 yr) <sup>-1</sup>	0.56	1.13	2.3	5.64
EUSO (3 yr) <sup>-1</sup>	3.0	6.0	12.2	30.0

Table 1: Number of events at 10<sup>19</sup> eV obtained for different detectors and periods of data collection. In the first two columns the calculation includes the finite extension of the atmospheric layer where the HORTAUs shower may take place and we adopted the most restrictive  $L_{\tau(\beta)}$  as the interaction length, while in the latter two columns we have neglected the presence of the atmosphere and we have used  $l_{\tau}$ . The assumed incoming neutrino fluence within the GZK or Z-burst model at energy 10<sup>19</sup> eV is  $\phi_{\nu} \simeq 50 \cdot E^{-1} \text{ eV cm}^{-2} \text{ s}^{-1} \text{ sr}^{-1}$

## 6. Conclusions

Horizontal and Upward  $\tau$  neutrinos emerging from the Earth and the consequent detection of  $\tau$  showers in air may represent an alternative way to investigate the neutrino astrophysics and possibly to open a Neutrino Astronomy at energies greater than 10<sup>15</sup> eV. The conversion of  $\tau$  neutrinos into  $\tau$  leptons coming out from a mountain chain (Fargion, Aiello, & Conversano 1999) or from the Earth (Fargion 2002a; Feng et al. 2002; Bertou et al. 2002) may lead to electromagnetic and hadronic showers producing an amplified signal of gamma,X,muon bundles, electron pairs and Cherenkov or fluorescent photons. Contrary to any downward  $\nu$  induced air-shower the detection of upward tau air-showers is not constrained by the presence of a high background noise. We present an exact analytical procedure to calculate the expected rate of up-going tau air-showers applied to the characteristics of large area detectors such as Auger and EUSO. We have introduced an effective volume and mass, which are independent of the neutrino fluxes, describing the Earth volume where neutrino-nucleon ( $\nu_{\tau} - N$ ) interactions may produce emerging  $\tau$

leptons. We have calculated such effective volume and mass taking into account the exact terrestrial structure, as a function of both the initial  $\nu_\tau$  and the final  $\tau$  energy (the latter being the only observable quantity). To obtain a realistic prediction of effective target volumes and masses we considered the  $\tau$  energy losses while propagating within the Earth and the atmosphere finite size where  $\tau$  might decay in flight. We prove the dominant role of HORTAUs and UPTAUs volume and mass respect to those of atmospheric layers in the very relevant range  $10^{16} - 10^{19}$  eV. Secondly, we show for the first time that when we consider a multi-layer structure of the Earth as predicted by Dziewonski (1989), the equivalent mass for an outer layer made of rock is dominant compared to the water, contrary to simplified all-rock/all-water Earth models (Figs. 10, 11, 13) and previous studies (Bottai & Giurgula 2003).

The EUSO space Observatory designed to detect UHECR may also discover HORTAUS and UPTAUS. We find that the effective HORTAUs-UPTAUs mass for water and rock in EUSO at  $10^{19}$  eV is  $780 \text{ km}^3$  and  $1600 \text{ km}^3$  water equivalent (and, at  $10^{18}$  eV,  $3.18 \cdot 10^3 \text{ km}^3$ ,  $8.48 \cdot 10^3 \text{ km}^3$  respectively). The average Earth mass observed by EUSO is  $1.02 \cdot 10^3 \text{ km}^3$ . Even considering the EUSO duty cycle efficiency as low as 0.1 these huge masses ( $\simeq 100 \text{ km}^3$ ) are making the EUSO telescope the widest neutrino future detectors at HORTAUs highest energies.

We show that neutrino signals may be well detected by EUSO, obtaining an event number rate at  $E_\tau = 10^{19}$  eV which is at least  $N_{ev}^{water} = 3.0 (\phi_\nu E_\nu / 50 \text{ eV cm}^{-2} \text{ s}^{-1} \text{ sr}^{-1})$  in the most conservative scenario assuming that the outer layer of the Earth is made of water ( $\rho_r = 1.02$ ). Moreover we find that  $N_{ev}^{rock} = 6.0 (\phi_\nu E_\nu / 50 \text{ eV cm}^{-2} \text{ s}^{-1} \text{ sr}^{-1})$ , for an outer layer relative density  $\rho_r = 2.65$ . The consequent average number of events in three years is  $\langle N_{ev} \rangle = 4.0 (\phi_\nu E_\nu / 50 \text{ eV cm}^{-2} \text{ s}^{-1} \text{ sr}^{-1})$ , obtained with a minimal WB97 or GZK neutrino flux  $\propto E^{-2}$ . If one considers the HORTAUs events partially contained in

the FOV of EUSO (see Fig. 12) they must be at least doubled. A lower energy threshold  $E_\tau \simeq 10^{18}$  eV in GZK models possible to achieve for Cherenkov diffused tracks, may lead to a significant increase of the event number up to an order of magnitude. Geo-magnetic bending of HORTAUs and UPTAUS at high quota will generally produce a fan-shaped shower " polarized " along the plane orthogonal to the direction of the local magnetic field. Such a signature, due to the magnetic splitting of the different components of the shower ( $e^\pm, \mu^\pm, \gamma$ ) may be detected by EUSO and its polarization axis is an additional criterion to distinguish such events. The more abundant HIAS (High Altitude Air-Showers), see Fig. 2, event rate even nearly one-two order of magnitude above HORTAUs rate, can not hide the HORTAUs events because of their characteristic downward signature (Fargion, Khlopov et al. 2003, Fig.32 ).

However UPTAUs (at PeV energies) arise at a negligible rate (even for an observing period of three years) because of the very narrow beam  $\Delta\Omega \simeq 2.5 \cdot 10^{-5}$  rad needed to point upward towards the EUSO telescope. Therefore the expected number of events is  $N_{eV} \simeq N_{Uptaus} \cdot \Delta\Omega/\Omega = 0.025$  for the water and  $N_{eV} \simeq N_{Uptaus} \cdot \Delta\Omega/\Omega = 0.08$  for the rock.

We also consider the possibility of detection of HORTAUS and UPTAUS with Auger, and according to our calculation we obtain with no duty cycle cut-off a number of events which is at  $E_\tau \simeq 10^{19}$  eV only slightly above the unity (see Fig. 19 and Table 1).

We find that our results differ from those of very recent studies (Yoshida et al. 2004, Bottai & Giurgola 2002). As regards Yoshida et al. (2004), shown in Fig. 20, we have obtained a number of events that is at least 3 times lower even in our less restrictive scenario, where the atmospheric layer has not been considered, and where we have used longest  $l_\tau$  as the interaction length. At energy band  $10^{16} - 10^{18}$  eV the discrepancy might be due to the fact that Yoshida et al. (2004) consider as a detection all those events where tau leptons propagate through the  $km^3$  volume. In our analysis instead, we consider only the

$\tau$ 's that are produced inside the thin layer (mainly defined by  $l_\tau$ ) just below the  $km^2$  and that are able to emerge from such a surface area. When we introduce the more realistic and restrictive  $L_{\tau(\beta)}$  interaction length and we take into account the presence of the atmosphere, our rate of events (now as a function of  $E_{\tau_f}$ ) at  $E_\tau \sim 10^{19}$  eV (see Table 1 and Fig. 20) is about 12 times lower than Yoshida and collaborators' one. At  $E_\tau \sim 10^{18}$  there is still a difference of about one order of magnitude between our (lower) and their (larger) event rate.

On the contrary, the comparison of our results with BG03 ones leads to a larger discrepancy in the opposite way. We infer that a standard rock outer layer provides a higher number (by a factor 2.6) of events compared to a layer made of water, while according to BG03 the efficiency of the two matter densities is inverted (by a factor larger than 2). Secondly the expected number of their events appears to be much more suppressed, by about two orders of magnitude, for both the water and the rock, assuming a GZK or a WB97 neutrino flux. The direct comparison between the results of BG03 and Yoshida and collaborators implies an even larger gap.

Finally we emphasize the evidence of an expected high number of events at energies  $E_\tau \lesssim 10^{19}$  eV. Therefore the most relevant Horizontal Tau Air-Shower, HORTAUs at GZK energies will be better searched and revealed at a lower threshold. These events may originate within a huge ring around the EUSO FOV whose surface is  $A \geq 6.6 \cdot 10^6 km^2$ . The horizontal  $\tau$ 's decay occur far away from such a ring ( $\geq 550$  km), inside the FOV of EUSO, and at high altitudes ( $\geq 20 - 40$  km), and they will give signatures clearly distinguishable from any other downward horizontal UHECR. Therefore we suggest (a) to improve the fast pattern recognition of Horizontal Shower Tracks to discriminate HIAS as well as HORTAU showers appearing as a sequence of dots with a forked signature; (b) to enlarge the Telescope Radius to reach energy thresholds lower than  $10^{19}$  eV where HORTAU

neutrino signals are enhanced, mostly in the optical wavelengths where Cherenkov photons are produced. (c) To improve the angular resolution within an accuracy  $\Delta\theta \leq 0.2^\circ$ , and the error on the measurement of the shower altitude to  $\Delta h \leq 2$ , km to better disentangle HIAS from HORTAUs. (d) to search for the HORTAUs enhancement along the highest density geological sites such as the highest volcanos, or mountain chains. Because of the better transparency of the water to  $\nu_\tau$  compared to the rock, such HORTAUs enhancement would be in principle more evident for largest mountain chains close to the sea. The most remarkable sites could be found in North America (Rocky Mountains), central America (Sierra Madre), but in particular the Andes mountains in South America, and the Indonesian Peninsula in Asia show the highest density contrast and they are bounded by massive submarine depths. These continental shelves must enhance greatly the HORTAUs rates. If the Auger experiment would improve horizontal shower resolution at low energy ( $\simeq 10^{18}$  eV), it may benefit of this natural rock barrier observing a peculiar East-West asymmetry (Fargion, Aiello, & Conversano 1999; Fargion 2002a; Bertou et al. 2002) at EeV energy band.

To conclude large effective volumes are necessary for neutrino detectors in order to reach useful sensitivity, given the extremely low flux and weak interactions of UHE neutrinos. We have shown that EUSO is a very promising mission because it allows to inspect HORTAUS from a large effective volume, of the order of a thousand (or because duty cycle, at least a hundred) cubic kilometers water equivalent. Other projects such as SALSA (Gorham et al. 2002a) and ANITA (Gorham et al. 2002b) have a large effective telescope area, corresponding to neutrino huge detection volumes nearly comparable with EUSO. But they are mostly neutrino collecting detectors with poor angular resolution. EUSO on the other hand can discriminate the directionality of the neutrino signatures, and as we have definitively proved, it has the ability to find out at least half a dozen of events when we assume the most conservative and guaranteed GZK neutrino flux.

## 7. Appendix

The final results we have presented in this paper have been first tested and constrained with the analysis of simpler approximate scenarios which we have used to set upper and lower bounds on our results. First if we consider the Earth as an homogeneous sphere made of water (or rock) one finds (Fargion 2002b, 2003):

$$\frac{V_{eff}}{A_{\oplus}} = \int_0^{\frac{\pi}{2}} \frac{(2\pi R_{\oplus} \cos \theta) l_{\tau} \sin \theta}{2\pi R_{\oplus}^2} \cdot e^{-\frac{2R_{\oplus} \sin \theta}{L_{\nu\tau}}} R_{\oplus} d\theta = \left(\frac{L_{\nu\tau}}{2R_{\oplus}}\right)^2 l_{\tau} \int_0^{\frac{2R_{\oplus}}{L_{\nu\tau}}} t \cdot e^{-t} dt$$

$$V_{eff-Max} = A_{Euso} \left(1 - e^{-\frac{L_0}{c\tau\tau\gamma\tau}}\right) \left(\frac{L_{\nu\tau}}{2R_{\oplus}}\right)^2 \cdot l_{\tau} \left[1 - e^{-\frac{2R_{\oplus}}{L_{\nu\tau}}}\left(1 + \frac{2R_{\oplus}}{L_{\nu\tau}}\right)\right] \quad (15)$$

while if we take into account only a thin outer layer of water (or rock) not deeper than  $4.5km$ , (considering all the inner terrestrial shells of infinite densities):

$$V_{eff-Min} = A_{Euso} \left(1 - e^{-\frac{L_0}{c\tau\tau\gamma\tau}}\right) \left(\frac{L_{\nu\tau}}{2R_{\oplus}}\right)^2 \cdot l_{\tau} \left[1 - e^{-\frac{2R_{\oplus} \sin(\theta_1)}{L_{\nu\tau}}}\left(1 + \frac{2R_{\oplus} \sin(\theta_1)}{L_{\nu\tau}}\right)\right] \quad (16)$$

Where  $\theta_1$  is the angle between the tangential plane to the surface of the Earth at the horizon and to the inner layer (ocean - rock) we are considering, and it is  $\theta_1 \cong 1.076^\circ$ .

The above geometrical quantities have been already defined in the text. It is possible to see that the effective volume in the low energy approximation reduces to:

$$V_{eff} = A_{Euso} \left(1 - e^{-\frac{L_0}{c\tau\tau\gamma\tau}}\right) \frac{l_{\tau}}{2} \quad (17)$$



This is the simplest result that may be derived in a direct way, and it guarantees a link between the most sophisticated analytical integral (Eq. 3) and the upper and lower bounds set by Eqs. 15 and 16.

Indeed, to calculate the effective volume in a more precise way one has to consider the Earth as a sequence of shells. For the first shell one obtains the same result as in Eq. 16.

$$\frac{V_1(E_\tau)}{A} = \frac{l_\tau}{\left(1 - \frac{l_\tau}{L_{\nu_{1w}}}\right)} \left(\frac{L_{\nu_{1w}}}{2R_\oplus}\right)^2 \left(1 - e^{-\frac{L_0}{l_{\tau 2}}}\right) \left[1 - e^{-\frac{2R_\oplus \sin \theta_1}{L_{\nu_{1w}}}} \left(1 + \frac{2R_\oplus \sin \theta_1}{L_{\nu_{1w}}}\right)\right]$$

For the following ones the corresponding volumes are given by

$$\frac{V_2(E_\tau)}{A} = \frac{l_\tau}{\left(1 - \frac{l_\tau}{L_{\nu_{1w}}}\right)} \left(1 - e^{-\frac{L_0}{l_{\tau 2}}}\right) \int_{\theta_1}^{\theta_2} d\theta \sin \theta \cos \theta \cdot e^{-2R_\oplus \left[ \left(\frac{\sin \theta - \sqrt{\cos^2 \theta_1 - \cos^2 \theta}}{L_{\nu_{water}}(E)}\right) + \left(\frac{\sqrt{\cos^2 \theta_1 - \cos^2 \theta}}{L_{\nu_{rock_1}}(E)}\right) \right]}$$

$$\begin{aligned} \frac{V_3(E_\tau)}{A} &= \frac{l_\tau}{\left(1 - \frac{l_\tau}{L_{\nu_{1w}}}\right)} \left(1 - e^{-\frac{L_0}{l_{\tau 2}}}\right) \int_{\theta_2}^{\theta_3} d\theta \sin \theta \cos \theta \cdot \\ &\cdot e^{-2R_\oplus \left[ \left(\frac{\sin \theta - \sqrt{\cos^2 \theta_1 - \cos^2 \theta}}{L_{\nu_{water}}(E)}\right) + \left(\frac{\sqrt{\cos^2 \theta_1 - \cos^2 \theta} - \sqrt{\cos^2 \theta_2 - \cos^2 \theta}}{L_{\nu_{rock_1}}(E)}\right) + \left(\frac{\sqrt{\cos^2 \theta_2 - \cos^2 \theta}}{L_{\nu_{rock_2}}(E)}\right) \right]} \end{aligned}$$

$$\frac{V_n(E_\tau)}{A} = \frac{l_\tau}{\left(1 - \frac{l_\tau}{L_{\nu_1}}\right)} \left(1 - e^{-\frac{L_0}{l_{\tau 2}}}\right).$$

$$\cdot \int_{\theta_{n-1}}^{\theta_n} d\theta \sin(\theta) \cos(\theta) \exp \left\{ -2R_0 \left[ \frac{\sin(\theta)}{L_{\nu_1}} + \sum_{j=1, n-1} \sqrt{\cos^2(\theta_j) - \cos^2(\theta)} \left( \frac{1}{L_{\nu_{j+1}}} - \frac{1}{L_{\nu_j}} \right) \right] \right\} \quad (18)$$

where again,  $\rho_{r_j}$  is the relative density of the matter respect to the water,

$$L_{\nu_j} = (n_{\rho_{r_j}} \sigma_{CC})^{-1}, \text{ and } \theta_j \equiv \arccos \frac{R_j}{R_\oplus}.$$

Thus the total effective volume is

$$\frac{V_{tot}(E_\tau)_{Shells}}{A} = \sum_{n=1,N} \frac{V_n(E_\tau)}{A} = \sum_{n=1,N} \frac{l_\tau \left(1 - e^{-\frac{L_0}{l_\tau}}\right)}{\left(1 - \frac{l_\tau}{L_{\nu_1}}\right)} \cdot \int_{\theta_{n-1}}^{\theta_n} \sin(\theta) \cos(\theta) \exp \left\{ -2R_0 \left[ \frac{\sin(\theta)}{L_{\nu_1}} + \sum_{j=1,n-1} \sqrt{\cos^2(\theta_j) - \cos^2(\theta)} \left( \frac{1}{L_{\nu_{j+1}}} - \frac{1}{L_{\nu_j}} \right) \right] \right\}$$

This result coincides with the analytic expression of the effective volume we have derived in the text using the  $D(\theta)$ . In this way we have calibrated the two methods and we have verified that they converge to a unique result when we calculate the effective volume, mass and event rate.

		$R_{j+1}(Km) > R > R_j(Km)$
$L_{\nu_{1w}} = L_{\nu_{water1}}$	$\rho_r = 1.02$	$6371 > R > 6368$
$L_{\nu_{1r}} = L_{\nu_{rock1}}$	$\rho_r = 2.65$	$6371 > R > 6368$
$L_{\nu_{2r}} = L_{\nu_{rock2}}$	$\rho_r = 2.76$	$6368 > R > 6346$
$L_{\nu_{3r}} = L_{\nu_{rock3}}$	$\rho_r = 3.63$	$6346 > R > 5700$
$L_{\nu_{4r}} = L_{\nu_{rock4}}$	$\rho_r = 5.05$	$5700 > R > 3480$
$L_{\nu_{5r}} = L_{\nu_{rock5}}$	$\rho_r = 11.28$	$3480 > R > 1221$
$L_{\nu_{6r}} = L_{\nu_{rock6}}$	$\rho_r = 12.99$	$1221 > R > 0$

### **7.1. Acknowledgment**

The author wish to thank Prof. Livio Scarsi for inspiring the present search as well as the EUSO collaboration for the exciting discussion; the author thanks M.Teshima for technical suggestions.

## REFERENCES

- Andres, E., et al. 2000, *Astropart. Phys.*, 7, 263
- Anselmann et al., [Gallex Collaboration], 1992, *Phys. Lett. B*, 285, 376
- Bhattacharjee, P., Hill, C.T. Schramm, D.N., 1992, *Phys. Rev. Lett.*, 69, 567B
- SNO Collaboration, 2002, *Phys.Rev.Lett.*, 89, 011302.
- Berezinsky, V.S., et al., 1990, *Astrophysics of Cosmic Rays* (North Holland ed.)
- Bertou, X., Billoir, P., Deligny, O., Lachaud, C., Letessier, S.A, 2002, *Astropart. Phys.*, 17, 183
- Bottai, S., Giurgola, S., 2003, BG03, *Astrop. Phys.*, 18, 539
- Bugaev, E.V., Montaruli, T., Sokalski, I.A., 2003, astro-ph/0311086
- Cronin, J.W., 2004, astro-ph/0402487
- Dziewonski, A., 1989, "Earth Structure Global" in *The Encyclopedia of Solid Earth Geophysics*, edited by D.E. James (Van Nostrand Reinhold, New York), p.331
- Dolgov, A., 2002, *Phys. Rept.* 370, 333, hep-ph/0202122
- Dubrovich, V., Fargion, D., & Khlopov, M., 2004, in prep.
- Dutta, I.S., Reno, M.H, Sarcevic, I., & Seckel, D., 2001, *Phys. Rev. D*, 63 094020
- Eguchi, et al., 2003, *Phys. Rev. Lett.*, 90, 021802
- Fargion, D., & Salis, A., 1997, Proc.25th ICRC HE-4-6153

- Fargion, D., Mele, B., & Salis, A., 1999, ApJ 517, 725; astro-ph/9710029
- Fargion, D., Aiello, A., Conversano, R., 1999, 26th ICRC HE6.1.10 396-398; astro-ph/9906450
- Fargion, D., Grossi, M., De Sanctis Lucentini, P.G., Di Troia, C., & Konoplich, R.V., 2000, in DARK2000, Heidelberg 10-14, July; Ed. Klapdor-Kleingrothaus H V Springer 2001, 455-468
- Fargion, D., Grossi, M., De Sanctis Lucentini, P.G., & Troia, C., 2001, J. Phys. Soc. Jpn., 70, 46
- Fargion, D., 2001a, 27th ICRC 2001 HE2.5 1297-1300, astro-ph/0106239
- Fargion, D., 2001b, 27th ICRC 2001 HE1.8 Germany 903-906, astro-ph/0107094
- Fargion, D., 2001c, JHEP PrHEP-hep2001/208; hep-ph/0111289
- Fargion, D., 2002a, ApJ, 570, 909; astro-ph/0002453; astro-ph/9704205
- Fargion, D., 2002b, SPIE Conference Proc. 4858, 1-13, hep-ph/0208093.
- Fargion, D., 2002c, Oulu, Beyond the Standard Model Conference; hep-ph/0211153
- Fargion, D., Khlopov, M., Konoplich, R., De Sanctis Lucentini, P. G., De Santis, M., and Mele, B., 2003, Recent Res. Devel.Astrophysics., 1
- Fargion, D., 2003, JHEP, PRHEP-AHEP 2003/031 astro-ph/0312627
- Feng, J.L., Fisher, P., Wilczek, F., & Terri, M. Yu, 2002, Phys. Rev. Lett. 88, 161102; hep-ph/0105067
- Fodor, Z., Katz, S.D., & Ringwald, A., 2002, Phys. Rev. Lett., 88, 171101; hep-ph/0210123
- Fukuda, Y. et al. [Super-Kamiokande Collaboration], 1998, Phys. Rev. Lett., 81, 1562

- Gandhi, R., Quigg, C., Reno, M.H., Sarcevic, I., 1996, *Astrop. Phys.*, 5, 81
- Gandhi, R., Quigg, C., Reno, M.H., Sarcevic, I., 1998, *Phys. Rev. D.*, 58, 093009
- Gorbunov, D., Tinyakov, P., Tkachev, I., & Troitsky, S., 2002, *ApJ*, 577, L93
- Grieder, P., et al., *Nucl. Phys. B (Proc. Suppl.)*, 97, 105
- Greisen, K., 1966, *Phys. Rev. Lett.*, 16, 748
- Hou, G.W.S., & Huang, M.A., 2002, *Proceedings of The First NCTS Workshop on Astroparticle Physics*, Kenting, Taiwan, Dec. 6-8, 2001; astro-ph/0204145
- Halzen, F., & Hooper, D., 2002, *Rept. Prog. Phys.*, 65, 1025
- Hayashida, N. et al., [AGASA collaboration], 1999, astro-ph/9906056
- Hou, G.W.S., & Huang, M.A., 2002, *Proceedings of The First NCTS Workshop on Astroparticle Physics*, Kenting, Taiwan, Dec. 6-8, 2001; astro-ph/0204145
- Jones, J., Mocioni, I., Reno, M.H., Sarcevic, I., 2004 *Phys. Rev. D* , 69, 033004
- Kalashov, O.E., Kuzmin, V.A., Semikoz, D.V., & Sigl, G., 2002 *Phys. Rev. D* 66 063004
- KamLand Collaboration, 2002, hep-ex/0212021.
- Klapdor-Kleingrothaus, H. V., Dietz, A., Harney, H.L., & Krivosheina, I.V., 2001, *Mod. Phys. Lett. A*, 16, 2409
- Mannheim K., Protheroe, R.J., Rachen, J.P., 2001 , *Phys.Rev.* D63 023003
- Montaruli, T. et al., [ANTARES collaboration] 2002, *Nucl. Phys. Proc. Suppl.*, 110, 513; hep-ex/0201009
- Raffelt, G.G., 2002, *New Astron.Rev.*, 46, 699, astro-ph/0207220

Semikoz, D., & Sigl G., 2003, hep-ph/0309328

Sigl, G., Schramm, D. N., Bhattacharjee, P., 1994, *Astropart. Phys.*, 2, 401

Sigl, G., 2002, *New Astron.Rev.*, 46, 699, astro-ph/0207220

Singh S., Ma C. P., astro-ph/0208419.

Takeda, M. and AGASA Collab., 2001, *J. Phys. Soc. Jpn.*, 70, 15

Tinyakov, P., & Tkachev, I., 2001, *J. Phys. Soc. Jpn.*, 70, 58

Uchihori, Y. et al., 2000, *Astropart.Phys.*, 13, 151

Yoshida, S., Sigl, G., & Lee, S., 1998, *Phys. Rev. Lett.* 81, 5505

Yoshida, S., Ishibashi, R., Miyamoto, H., 2003, *Phys. Rev. D*, accepted ; astro-ph/0312078

Waxman, E., Bachall, J., 1997, *Phys. Rev. Lett.*, 78, 2292

Weiler, T.J., 1999, *Astropart. Phys.* 11, 303

Zatsepin, G.T., & Kuz'min, V.A., 1966, *JETP Lett.* 4, 78.